

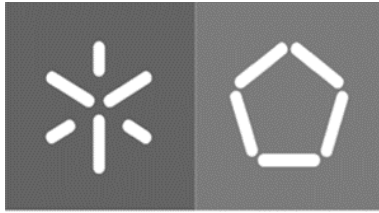


Universidade do Minho
Escola de Engenharia

Filipa Alves Mendonça Pereira

**Development of Stretchable and
Conductive 3D Printed Sensor
Structures for Washable Textile
Applications**





Universidade do Minho
Escola de Engenharia

Filipa Alves Mendonça Pereira

**Development of Stretchable and
Conductive 3D Printed Sensor Structures
for Washable Textile Applications**

Dissertação de Mestrado
Mestrado Integrado em Engenharia Têxtil

Trabalho efetuado sob a orientação de
**Professor Doutor Maria José Araújo Marques
Abreu**
Professor Doutor Anne Schwarz-Pfeiffer

Julho de 2021

DIREITOS DE AUTOR E CONDIÇÕES DE UTILIZAÇÃO DO TRABALHO POR TERCEIROS

Este é um trabalho académico que pode ser utilizado por terceiros desde que respeitadas as regras e boas práticas internacionalmente aceites, no que concerne aos direitos de autor e direitos conexos.

Assim, o presente trabalho pode ser utilizado nos termos previstos na licença abaixo indicada.

Caso o utilizador necessite de permissão para poder fazer um uso do trabalho em condições não previstas no licenciamento indicado, deverá contactar o autor, através do RepositóriUM da Universidade do Minho.



Atribuição-NãoComercial-SemDerivações
CC BY-NC-ND

<https://creativecommons.org/licenses/by-nc-nd/4.0/>

ACKNOWLEDGEMENTS

Above all else, I want to thank my parents and my brother for all the support given during this dissertation and throughout my academic career and specially for the effort and sacrifices they made so that I could get here. This work is also theirs.

To my advisor, Professor Maria José Abreu, whose contribution was fundamental to the conclusion of this project. I am grateful for all the dedication and effort that you showed right from the start and for the time available to clarify any doubts that had arisen.

To Professor Anne Schwarz-Pfeiffer of Hochschule Niederrhein, who was always available during my stay in Mönchengladbach and helped me choose the final theme despite the constant changes caused by factors external to the work.

To colleague Ramona Nolden, to whom I owe a thousand thanks for the daily company and always helping me to solve the constant arising problems. This work would not be possible without her support and amazingly contagious energetic mood that helped me overcome all the obstacles.

To professor António Pedro Souto, I would like to thank all the moments that inspired me to become a better student and future professional. Having him as a teacher was a huge pleasure, this work is also the result of his influence.

To my grandparents and uncles, a thank you for building a family dynamic where I always felt supported, and which allowed for growth at a personal and academic level.

To my friends, who made my academic adventure a dream come true, without them these six years would not have the same meaning.

To my boyfriend, I would like to thank all the patience and support during this journey.

Thank you all!

STATEMENT OF INTEGRITY

I hereby declare having conducted this academic work with integrity. I confirm that I have not used plagiarism or any form of undue use of information or falsification of results along the process leading to its elaboration. I further declare that I have fully acknowledged the Code of Ethical Conduct of the University of Minho.

A rectangular box containing a handwritten signature in blue ink. The signature reads "Feipa Pereira".

ABSTRACT

This dissertation project arises from the need to monitor patients after a total knee operation, using an intelligent elastic band. The specific aim of this work is to evaluate the influence of parameters, such as cross-sectional area and pattern, on elastic conductors for e-textile applications. For this purpose, a 3D printer capable of printing a conductive paste with different print diameters was used, using five different designs. The substrate used for the printing was a polyurethane film, as it is close, in terms of elasticity, to textile substrates. In terms of testing, the electrical resistance was kept as an analysis reference since it is inversely proportional to conductivity. The samples were subjected to a maximum stretch of 10% and the collected values were analyzed before and after a domestic washing cycle. The results allowed to conclude that an increment of the cross-sectional area is inversely proportional to the sample's resistance and that the washing process negatively affects its resistance. It was not possible to make any final conclusions on the influence of the pattern on the sample's resistance. This work serves as a database for future work.

Keywords: e-textiles; conductive paste; 3D printing; flexible conductors

Resumo

Este projeto de dissertação surge da necessidade de monitorizar pacientes após uma operação total ao joelho, através de uma banda elástica inteligente. O objetivo específico deste trabalho é a avaliação da influência de parâmetros, como a área transversal e o padrão, em condutores elásticos para aplicações em e-têxteis. Para tal, foi utilizada uma impressora 3D capaz de imprimir uma pasta condutora com diferentes diâmetros de impressão, utilizando cinco designs distintos. O substrato utilizado para a impressão foi um filme de poliuretano, uma vez que se aproxima, em termos de elasticidade, de substratos têxteis. Em termos de testagem, a resistência elétrica foi mantida como referência de análise uma vez que é inversamente proporcional à condutividade. As amostras foram submetidas a uma estiragem máxima de 10% e os valores recolhidos foram analisados antes e depois de serem submetidos a uma ação de lavagem doméstica. Os resultados permitiram concluir que o aumento da área transversal é inversamente proporcional à resistência das amostras e que o processo de lavagem afeta negativamente a sua resistência. Não foram possíveis retirar conclusões finais acerca da influência dos padrões na resistência das amostras. Este trabalho serve como uma base de dados para trabalhos futuros.

Palavras-chave: e-têxteis; pasta condutiva; impressão 3D; condutores flexíveis

TABLE OF CONTENTS

ACKNOWLEDGEMENTS.....	i
STATEMENT OF INTEGRITY.....	ii
ABSTRACT.....	iii
RESUMO.....	iv.
TABLE OF CONTENTS.....	v
FIGURE LIST	viii
TABLE LIST	x
ABREVIATION LIST.....	xi
1 INTRODUCTION	1
1.1 Objectives and Obstacles.....	2
1.2 Overview of the Structure	3
2 LITERATURE REVIEW	5
2.1 E-textiles.....	5
2.1.1 Sensors	6
2.1.2 Conductive Materials	8
2.1.3 Coating	9
2.2 Manufacturing Processes.....	11
2.2.1 Screen Printing	11
2.2.2 Digital Printing.....	12
2.2.3 3D Printing.....	13
2.3 Printed Patterns for Conductive Applications	16
2.3.1 Reliability of Roll-to-roll-printed, flexible electrodes for e-clothing applications	16

2.3.2	Printable stretchable silver ink and application to printed RFID tags for wearable electronics	18
2.3.3	Bending reliability of printed conductors deposited on plastic foil with various silver patterns	19
2.3.4	General Conclusions	21
2.4	Electrical Properties	21
2.4.1	Ohm’s Law	21
3	METHODOLOGY	23
3.1	Preparation of Samples.....	23
3.2	Methods of Data Collection	29
4	RESULTS AND DISCUSSION	31
4.1	Characterization of the Samples.....	31
4.1.1	Silver Flakes Dimensions Values.....	31
4.1.2	Cross-sectional Area of the Printed Samples	32
4.1.3	Theoretical Resistance Values for the Produced Paste.....	34
4.1.4	Length of the Samples.....	35
4.2	Results from the Stretching Analysis	36
4.3	Printing Trials of the Linear Patterns	38
4.3.1	A1 samples	38
4.3.2	B1 samples	39
4.3.3	Comparison of the Linear Samples Printed with the Two Nozzles ...	39
4.4	Printing Trials of Larger Rectangular Pattern	40
4.4.1	A2 samples	40
4.4.2	B2 samples	41
4.4.3	Comparison of the Larger Rectangular Samples Printed with the Two Nozzles	42

4.5	Printing Trials of Smaller Rectangular Pattern	42
4.5.1	A3 samples	42
4.5.2	B3 samples	43
4.5.3	Comparison of the Smaller Rectangular Samples Printed with the Two Nozzles	44
4.6	Printing Trials of Larger Circular Pattern	44
4.6.1	A4 samples	44
4.6.2	B4 samples	45
4.6.3	Comparison of the Larger Circular Samples Printed with the Two Nozzles	46
4.7	Printing Trials of Smaller Circular Pattern	46
4.7.1	A5 samples	46
4.7.2	B5 samples	47
4.7.3	Comparison of the Smaller Circular Samples Printed with the Two Nozzles	48
4.8	General Conclusions	48
5	CONCLUSION	52
5.1	Limitations and Future Work	54
	REFERENCES	55
	ANNEX	58
	Polyurethane film “Platilon U 9122” Data Sheet	58
	eConduct Glass 352000 Data Sheet	60
	Elastosil® LR 6200 A/B Data Sheet	61
	TUBICOAT PU 60 Data Sheet	64
	TUBICOAT Verdicker LP Data Sheet	66

FIGURE LIST

Figure 1 - Piezoresistive pressure sensor operating principle (Avnet Abacus, 2019)	8
Figure 2 – Example of Screen Printing Process (Jaime, 2010).....	11
Figure 3 - Fluids emerging from a nozzle (images courtesy of Xennia Technology Ltd): (a) dripping faucet; (b) drop on demand; (c) continuous ink jet; (d) atomisation	13
Figure 4 - 8 different patterns used by R. Silz et. al.	17
Figure 5 - Screen printing pattern used by Zhong et. al.....	18
Figure 6 - Set of 5 patterns printed by T. Happonen, T. Ritvonen, P. Korhonen et al....	20
Figure 7 – Procusini machine.....	24
Figure 8 - Procusini producing samples.....	24
Figure 9 - Accumulation of silicon at the end of the printed lines	25
Figure 10 - Alternative screw top view.....	25
Figure 11 - Alternative screw front view	25
Figure 12 - Schematic of the methodology	28
Figure 13 - Resistomat Burster 2316 while measuring a sample	29
Figure 14 - Sample holding	30
Figure 15 - x50 amplification of a linear sample with 7 flakes differentiated	32
Figure 16 – Example of a x100 amplification of the cross-sectional area of a linear sample with silicone.....	33
Figure 17 - Cross-sectional area of nozzle A samples.....	34
Figure 18 - Cross-sectional area of nozzle B samples.....	34
Figure 19 - Reliability analysis of all samples before and after washing.....	37
Figure 20 – A1 samples.....	40
Figure 21 – B1 samples.....	40
Figure 22 – A2 samples.....	42
Figure 23 – B2 samples.....	42
Figure 24 – A3 samples.....	44
Figure 25 – B3 samples.....	44
Figure 26 – A4 samples.....	46
Figure 27 – B4 samples.....	46

Figure 28 - A5 samples.....	48
Figure 29 - B5 samples.....	48
Figure 30 - Comparison of B4 samples over stretching before and after washing.....	49
Figure 31 - Comparison between five patterns printed with nozzle A before washing	50
Figure 32 - Comparison between five patterns printed with nozzle B before washing.	50

TABLE LIST

Table 1 - The resistance of the produced screen-printed stretchable ink of article 2 (Zhong et al., 2019).....	19
Table 2 - Recipe for the conductive paste	26
Table 3 - Specifications of the different components of the conductive paste	26
Table 4 - Settings for the printing.....	27
Table 5 - Schematic of the 5 patterns	28
Table 6 - Theoretical lengths values of the samples	36
Table 7 - Simplified nomenclature for the different patterns.....	37
Table 8 - Reliability analysis of all samples before and after washing	37
Table 9 - Results from stretch testing of A1 samples	38
Table 10 - Results from stretch testing of B1 samples	39
Table 11 - Results from stretch testing of A2 samples	41
Table 12 - Results from stretch testing of B2 samples	41
Table 13 - Results from stretch testing of A3 samples	43
Table 14 - Results from stretch testing of B3 samples	43
Table 15 - Results from stretch testing of A4 samples	45
Table 16 - Results from stretch testing of B4 samples	45
Table 17 - Results from stretch testing of A5 samples	47
Table 18 - Results from stretch testing of B5 samples	47
Table 19 - Summary of resistance results	48

ABBREVIATION LIST

AM	Additive Manufacturing
AW	After Washing
BW	Before Washing
CAD	Computer Aided Design
CAM	Computer Aided Manufacturing
CNC	Computer Numerical Control
MS	Maximum Stretch
PCB	Printed Circuit Board
R	Resting
R2R	Roll-to-roll
STL	Standard Tessellation Language
UV	Ultraviolet

1 INTRODUCTION

The present dissertation is part of the study plan of the Integrated Master's in Textile Engineering at the University of Minho, and a representation of the final course project for the master's degree of student Filipa Alves Mendonça Pereira, in which it is intended to evaluate different conductive structures for textile applications.

This study arises from the need to efficiently monitor patients undergoing a total knee replacement surgery, also known as arthroplasty. In this type of surgery, health care is not limited to the time spent in the hospital, continuous monitoring and surveillance is necessary, reflecting in additional health costs.

Post-operation monitoring options are often associated with physical therapy sessions or appointments at specialized clinics, where there is no daily post-operation knee control. In most cases, this type of therapy does not incorporate the patient's daily activities such as climbing stairs or walking on an inclined floor. The difficulties that emerge in this type of activities can lead to a reassessment of the patient's needs at an early stage. Nevertheless, there are some alternatives that allow a more complete monitoring of the recovery. These are based on biomechanical or biomotion measurement systems, which can be derived from optical motion tracking or video image sequences (Atallah et al., 2011). However, these options also depend on specialized clinics or laboratories.

A recent alternative to this type of observation is self-monitoring devices. Some of these devices are already known among the public, such as *Nike+ Fuelband* or *Fitbit*. The principle of these accessories is the track of steps and calories burned during day. The data is obtained through wearable devices and the information is extracted digitally through smartphones or tablets. This concept can be entirely reused for medical purposes, reducing the need for a third party in the recovery process and consequently, reducing costs.

Due to these factors, the interest in e-textiles is increasing. The incorporation of sensors that measure the user's position, temperature and physical effort represents a mean of responding to the needs of self-monitoring devices intended for medical recovery. These

devices can be produced in two different ways: through classic electronic devices embedded in clothing, such as buttons, or by incorporating these components directly into the textile substrate. Either way, the connection between the different components represents a crucial element for the proper functioning of the e-textile.

Considering this panorama, the present work emerges as a study of the effect of different variables in the production of stretchable conductors. Its practical component was carried out at Hochschule Niederrhein in Mönchengladbach, Germany, during an Erasmus exchange program between february and august 2020, which main goal was the development of an intelligent knee bandage that could measure and monitor the movement of a knee after an operation through the optimization of a sensor embedded in a bandage material.

Textile structures are suitable for this purpose once they retain their strength, flexibility, comfort and durability and enable the integration of electronical devices such as sensors. The individual objective was initially based on the understanding of the machine *Squink* from the *Botfactory* company, along with the printing of circuit boards, PCB, onto textiles. However, some problems associated with connection and software did not made this possible. In order not to deviate a lot from the original plan, another 3D printer, *Procusini*, was used to analyse and compare different samples of conductive paste.

1.1 Objectives and Obstacles

The contribution of this individual work to the overall research project was the study of the feasibility of printed structures on the surface of textiles instead of incorporating them in their production. The results obtained will serve as a database for future work.

The main purpose of this work is to analyze different conductive samples by changing parameters such as pattern and cross-sectional area, and to conclude which one best fits the wanted results for the final product. To do so, five different printing patterns were applied, and two nozzle sizes were tried. The samples were then submitted to stretching forces and washing to simulate their behaviour during use.

With a view to organize the work throughout the months, a monthly planned schedule was made. This included the exploration of all the theoretical concepts associated with the final theme, the required experimental procedures that would be done in order to test and prove the studied theory, and the time to finish the written assignment. Unfortunately, due to the spread of a pandemic, commonly named as *Covid-19*, some changes had to be made and the schedule previously proposed was not followed. As a result of the circumstances, the practical work only began at the month of July which influenced the depth of the work originally designed. Nevertheless, the final goal was accomplished with a lot of effort and thanks to a various of very competent people.

At the start of the work, the two most studied subjects were related to e-textiles and 3D printing. In terms of additive manufacturing, or 3D printing, the research was based on type of machinery and their working principle, and how the printing parameters would affect the final print. Ultimately, it was also necessary to understand the basic concept of Ohm's law in order to better comprehend the results and hypothesize the possible reasons for certain outcomes.

In terms of methodology, quantitative methods were applied since they are more suitable for measuring and identifying patterns. This way it is possible to assemble generalizable knowledge about the elements being studied, different variables can be controlled, and conclusions will have stronger validation. All the results were gathered through experimental procedures.

1.2 Overview of the Structure

This dissertation consists of 5 chapters and a brief review of each chapter is presented below.

In **chapter 1**, the developed theme is introduced, presenting the topic, its relevance to the project and the main objectives and obstacles.

Chapter 2 refers to the literature review, where an overview of the current knowledge related to the selected topic is presented. This was achieved by reading various publications, books and scientific articles. The selected themes are crucial for a deep

understanding of the chosen theme and the keywords being, e-textiles, additive manufacturing and Ohm's law. To complement the contents exposed, some selected articles are analyzed in depth, allowing to establish expectations of the results to be obtained and formulate ideas about them.

The methodology of the work is presented in **chapter 3**, explaining point by point how the samples were produced, how the data was collected and analyzed and what materials were used throughout the process. This chapter allows the readers to evaluate the reliability and feasibility of the presented work.

Chapter 4 includes the presentation of all the results obtained, as well as the discussion. In this chapter, the research findings were reported through the mean and standard deviation of ten sample sets. The samples were compared between two nozzles and between different patterns. In order to facilitate the understanding of the results, several graphs and charts are used. Before interpreting the results, a characterization and a prediction of their theoretical values was also made in **chapter 4**.

Finally, **chapter 5** presents the conclusions obtained from the developed work, highlighting aspects to improve in future work.

2 LITERATURE REVIEW

2.1 E-textiles

In a society progressively connected to technology, the production of efficient e-textiles is extremely necessary and, consequently, studies related to the optimization of these products are increasing in recent years. There are two similar concepts used in the field of wearable electronics, smart textiles and e-textiles. A smart textile is a textile that reacts to an outside stimulus (heat, chemicals, magnetism or mechanical stimulus) but doesn't necessarily has an electronic component (European Committee for Standardization, 2011). On the other hand, e-textiles combine traditional textiles with electronic components enabling data transfer, for example through sensors.

In terms of production, the increasing interest in these products is due to the fact that they offer advantages such as low manufacturing costs, long-time endurance, sustainable production methods, lower energy consumption and higher efficiency (S. Merilampi et al., 2009). In addition to this, the electronic components can be integrated into the textile structures and not connected as a separated element.

Medical application is one of the main reasons for the increment of studies in this area. As an example, e-textiles can be used to monitor patients after operation or even, to analyze a person's performance during physical tests. Their constant contact with the body, makes flexibility and adaptability the main requirements for these products. These devices are subjected to various mechanical deformations including twisting, bending, folding, and stretching during operation (Zhong et al., 2019). As a result, the ultimate goal supporting research and development in this field is their ability to withstand deformations without limiting its handling (Sliz et al., 2020).

Currently, the most common method to prototype and fabricate e-clothing is to combine rigid components with stretchable interconnecting conductors. For this matter, stretchable conductors are interesting because they can tolerate large mechanical deformations, since the structure itself will deform without immediately breaking (Sari Merilampi et al., 2010), and still allow the transmission of signals during use. Therefore, the

role of reliable conductive elements and interconnections is substantial for further development of flexible electronics (Sliz et al., 2020).

In contemplation of obtaining efficient stretchable conductors, there are three parameters that can be changed and consequently achieve distinct results: these are the materials, the structure design and the application method. Another important aspect to consider when choosing the parameters is the temperature which the textile is submitted to when curing. Because of this, a lot of materials and methods are excluded since the required temperatures are too high and might compromise the textile structure.

2.1.1 Sensors

The most appealing trait for the sensors' applications in health and environmental monitoring, is by far the flexibility. In health monitoring, the ability to place sensing elements directly on the skin or to implement them into the clothing is key. Being able to move together with the measured subject without limiting or obstructing its manoeuvrability is the main goal supporting the research and developments in this field (Sliz et al., 2020).

Certain functionalities, such as sensing, can be combined with textile substrates by intrinsic and/or extrinsic modifications of the fabric. A pressure sensor contains a mechanism or structure that reacts proportionately to an applied force. After detecting and quantifying the effects of the applied pressure, the sensor produces an output that cannot be transferred directly to an electronic circuit. The physical response needs to be translated into an electrical signal, and then, conditioning is required in order to transform the analog signal into digital and usable.

The type of sensors used for e-textiles are normally miniaturized versions of conventional elements which are then inserted intrinsically into the fabric or attached to small supplementary components, like buttons or sequins. Theoretically, in terms of e-textiles, any kind of sensor which is sufficient compliantly, compact, lightweight, and 'adaptable' can be incorporated into fabrics (Castano & Flatau, 2014). The sensing properties that can be achieved are divided in four categories depending on the physical nature of

the sensor, which can be capacitive, resistive, optical and solar, being the most common capacitive and resistive. In adapted electronics, e-textiles employ conventional capacitors that are attached to fabrics using customized methods (Castano & Flatau, 2014). On the other hand, resistive sensor can be manufactured at all fabric structure levels, like yarn, fiber or coatings.

The reliability of e-textiles depends on the effectiveness of signal transmission between the different components, therefore, the improvement of the conductive connections in the textile substrate are essential for a proper functioning. Typically, conductive lines are established by manually attaching conventional wires or sewing conductive thread, replacing nonconductive fibers with conductive ones. Other common techniques are machine embroidering of conductive thread, and printing rigid and stretchable conduction lines using macroelectronics and microelectronics procedures (Castano & Flatau, 2014).

In recent literature, the most common interconnectors used for this purpose are conductive yarns. These can be created by combining conductive threads with non-conductive, by coating fibers with different kinds of metals or even by spinning threads from conductive materials. The use of conductive yarns represents a mechanical and physical technique of bonding connectors that can be difficult to accomplish due to machinery compatibility. Fortunately, some improved techniques, which include the use of conductive pastes, are beginning to achieve good results in terms of efficiency, and resolving some problems associated with usability.

An example of sensors that are used to build products based on pressure forces, are the piezoresistive sensors. In piezoresistive sensors, the pressure is measured by the analysis of fluctuation of the electrical resistance of a conductive material when deformed. Once the change in the resistance is directly proportional to the strain caused by pressure on the diagram (Avnet Abacus, 2019), it is possible to obtain very accurate and precise values. A schematic of the operating principle of these sensors is shown in Figure 1.

Even though these sensors have advantages, like being robust and have a stable performance and calibration, over time, they consume more power when compared to

others, not being advised to use them on battery powered or portable systems (Avnet Abacus, 2019).

The materials used in piezoresistive sensors are most commonly semiconductors, being the most common the silicon, and elastomers. Even though many materials show piezoresistivity characteristics, only those with high sensibility are suitable for such sensors. When a material does not have piezoresistive characteristics, adding conductive materials, such as carbon particles, to the non-conducting elastic material gives it the wanted characteristics (Regtien, 2012).

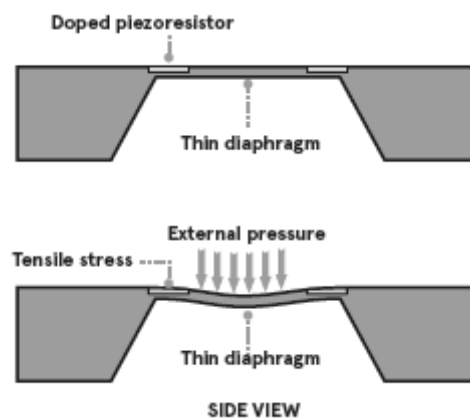


Figure 1 - Piezoresistive pressure sensor operating principle (Avnet Abacus, 2019)

2.1.2 Conductive Materials

The choice of the materials to be used as the conductor is extremely important as it is the parameter that will most affect the behavior of the e-textile. Since there is a need to combine conductivity with adaptability, the production of conductive patterns can be achieved by applying conductive particles in non-conducting inks or pastes. There are several materials that can be used towards this end, such as carbon nanotubes, silver or copper nanoparticles, elastomers (Sliz et al., 2020) and even liquid metal in some cases (Zhong et al., 2019) but, there is always a minimum filler content to ensure the conductivity of the polymer. In terms of performance, the aspects that influence the results are the shape, size and the distribution of the nanofillers, the interactions between them and the processing methods selected. Apart from this, there is also a list of considerations that need to be attended to have optimal results, like the unwanted agglomeration of

the nanofillers, its flexibility, mechanical strength, stiffness and chemical resistance. Additionally, the printing parameters should be carefully chosen because if the temperature is too high or the time at the hot end of the printer is too long, polymer degradation may occur, causing voids in the printed structure and contribute to lower electrical conductivity (Gnanasekaran et al., 2017). Nevertheless, the use of these materials may open new doors in the innovation process since they play an important part in recent discovers and studies.

2.1.3 Coating

Coating processes are defined by the application of a semi liquid material to one or both sides of a textile material. Once the coating has been dried (and cured, if necessary), it forms a bond with the fabric (Meirowitz, 2016).

Most coatings operations follow four different stages: the substrate preparation, the coating formulation along with its application and lastly, the postprocessing, which, as well as the first step, can be optional and should only be used if necessary. In order to obtain a surface with ideal initial characteristics, the fabric may be pre-treated through an aqueous or solvent scour, a caustic etch or plasma ablation. Similarly, after coating, the material can suffer curing, toughening the polymer material by cross-linking its chains.

Amongst a list of parameters that influence the efficiency of the interactions of the fabric and the coating, the most considerable are the adhesion between them and the wetting of the material. The adhesion depends on the intermolecular forces between both materials which can be divided into actual bonds (ionic and covalent) and weaker intermolecular forces (hydrogen bonding, dipole-dipole, induced dipole-dipole interactions and disperse forces) (Meirowitz, 2016).

There are other parameters that intrinsically effect the productivity of the coating process and even though they are not usually discussed, they alter the result. These parameters consist on the batch size, where the largest batches are preferred since they are more cost-efficient, the machine direction, which affects the strength, elongation,

tendency to crease, degree of edge curl or the friction of the fabric, and the cleanliness of specific particles (Meirowitz, 2016).

The traditional coating methods can be subdivided into groups. In free withdrawal process, the fabric is run through a bath full of coating formulation where the weight and thickness of the coating are influenced by the line speed, the rheology of the liquid and the interaction with the fabric (Meirowitz, 2016). Other possibilities are based on a metered or constrained flow process in which rolls are used to achieve metering or overexact coating, wherein the exact amount of coating is directly applied onto the fabric.

Once the interest in e-textiles seems to be exponentially growing over the years, it is important to develop improvements in the technology that makes it possible. In numerous areas of the industry, the functionalization of materials represents a major problem that can be addressed with simple solutions such as new coated materials. To do so, specific processes have emerged, and it is now possible to produce yarns or fabrics with properties that would not be conceivable without it. Among countless possibilities, chemical vapor deposition and dip-coating seem the most promising. Chemical vapor deposition is a synthesis process in which the chemical constituents react in the vapor phase near or on a heated substrate to form a solid deposit (Pierson et al., 1999). With semiconductor yarns as the outcome, this vapor coating process is a result of seven separate reactions: thermal decomposition, reduction, hydrolysis, disproportionation, oxidation, carbonization and nitridation. In this procedure, the most common materials that suffer deposition are silicon and carbon, which, go accordingly with what was initially established. In the dip-coating technique, the withdrawal of a substrate comes from a fluid sol: gravitational draining and solvent evaporation, accompanied by further condensation reactions, resulting in a deposition of a solid film (Brinker et al., 1991). The advantages of this method are based on its ability to adapt the microstructures of the deposited film and the need for less equipment and less expensive materials.

2.2 Manufacturing Processes

2.2.1 Screen Printing

Screen printing is a process used for transferring a design onto a flat surface using a mesh screen, paste and a squeegee (Figure 2). Even though it is a relatively simple technique, it requires multiple processing steps, cleaning of the screen and a great amount of paste goes to waste (Shahariar et al., 2019). Another disadvantage is that it alters the touch of the substrate that is being printed on and it can easily crack and lose the functionality by the mechanical deformation of textiles (Shahariar et al., 2019).

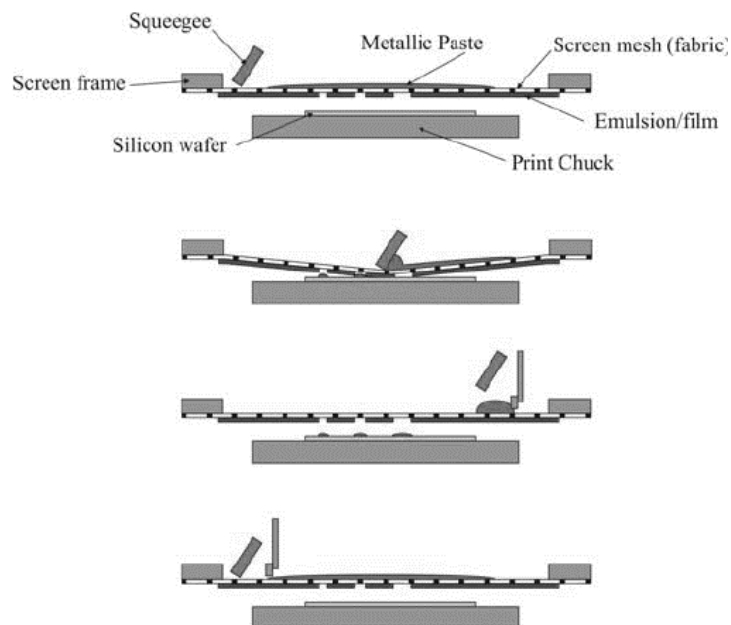


Figure 2 – Example of Screen Printing Process (Jaime, 2010)

Regarding the use of conductive pastes while using screen printing, the resistance of the printed patterns increases upon stretching because cracks are created which consequently leads to electric breakdown. This effect can be mitigated by using pastes with bigger particles, like for example silver flakes. In this process, silver flakes show better results than silver nanoparticles due to their flat shapes and large contact area between them (Zhong et al., 2019).

2.2.2 Digital Printing

Since its first appearance in the 1970s, digital printing has come a long way in terms of efficiency and technology and now represents a versatile and high-speed process that is exponentially growing in the textile sector (David J. Tyler, 2005).

There is a great deal of advantages on using digital printing in comparison with other traditional processes. For examples, in digital printing there are no restrictions on the file size used as the pattern, allowing more complex designs and, through the cyan–magenta–yellow–black color gamut, thousands of colors can be printed without the requirement for a color kitchen (D.J. Tyler, 2011a). Since it is possible to use a variety of inks, they can be customized to be compatible with any substrate and as there are no moving parts, it is the ink that moves during printing and not a mechanical device (D.J. Tyler, 2011a). There is no contact with the textile substrate, making it possible to print in substrates with different characteristics. Regarding the process enhancement, the use of printing technologies brought innovation in a way that it is now possible to have customized products with a reduced processing time, producing less waste and contributing to the production of small batches and therefore no stock storage, which, altogether, results in a lower operation cost (Dearden et al., 2005).

Among the different technologies currently available on the market, drop on demand, continuous inkjet and atomization are the standard approaches used by the industry (Figure 3). With reference to its basic operation (deposition of dye on surfaces) these techniques usually rely on water-based inks to produce proper resolutions and to ensure the drop of the ink on the substrate in a predetermined position. Generally, inks comprise a colorant, a carrier base and various additives (D.J. Tyler, 2011b). Ideally, water stands as the optimal carrier since it evaporates easily and due to its non-toxic essence.

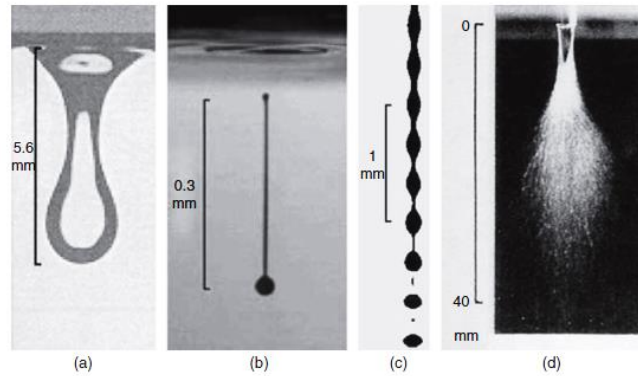


Figure 3 - Fluids emerging from a nozzle (images courtesy of Xennia Technology Ltd): (a) dripping faucet; (b) drop on demand; (c) continuous ink jet; (d) atomisation

Despite its advantages, applying this process in the creation of conducting patterns can become a challenge since nanoparticle-based conductive inks frequently cause blockage/clogging of inkjet printer nozzles (Shahariar et al., 2019). Also, due to the porosity and irregularity of the textile materials, it is sometimes necessary a large number of print passes since high-density metal particles are needed to create a conductive path (Shahariar et al., 2019). However, this can affect characteristics such as the touch and drape of the fabric or knitting.

2.2.3 3D Printing

At present day, there is a notorious growth of interest in the industry of additive manufacturing (AM) since it brings numerous advantages in terms of time and cost reduction. It enables customized prototyping and brings new advantages such as the ability to design non-conventional shapes and allows the prototype development with less time and involved resources. Therefore, it facilitates the use of different designs or models with the utilization of different software such as computer-aided design (CAD), computer-aided manufacturing (CAM) and computer numerical control (CNC) (Wong & Hernandez, 2012).

3D printing is an additive manufacturing technique for fabricating a wide range of structures and complex geometries from three-dimensional model data (Ngo et al., 2018). This emerging technology can be used in several industries such as construction,

biomedical, aerospace and represents an innovative way to produce prototypes or products with less waste and with freedom for design and automation, decreasing the costs of production and allowing the manufacture of unique and customized items. On the other hand, it brings certain disadvantages like the inferior mechanical properties associated with, and an anisotropic behavior. Also, the high costs and time-consumption of the AM process remain to be major hurdles that inhibit mass production (Ngo et al., 2018).

Another similar area of interest is micro-additive manufacturing technologies where the focus is upon microproducts and microfabrication. The major issues about microproducts are centralized in the use of different materials and in the design of complex 3D microstructures with high aspect ratios (Vaezi et al., 2013). Although there are different ideologies about the differences between micro-additive manufacturing processes, an intuitive definition is the division into three groups: the scalable AM technologies, the 3D direct printing or hybrid processes. From the vast list of possibilities, the most promising ones are based on laser chemical vapor deposition, focused ion beam and electrochemical fabrication. Due to the present tendency towards miniaturization of products in many industries comprising medical, automotive, optics, electronics, and biotechnology (Vaezi et al., 2013) there is an interest in studying and developing this manufacturing possibilities.

All the methods imply the previewed treatment with a CAD software and consequent transformation into a STL (Standard Tessellation Language) file. The STL file represents the standard file for this kind of application and transforms the earlier version of the design in different layers, containing the information of each layer. There are two parameters that are influenced by the selected equipment, this being the resolution and thickness of each layer.

2.2.3.1. Stereolithography

It is a liquid-based process that consists in the curing or solidification of a photosensitive polymer when an ultraviolet laser makes contact with the resin (Wong & Hernandez, 2012). It has a moving platform that is lowered after each finished layer and it is produced

through photopolymerization, a process where a liquid monomer instantly converts into polymer chains through UV activation. The UV acts as a catalyst for the reactions, also known as ultraviolet curing (Wong & Hernandez, 2012). After polymerization, a pattern inside the resin layer is solidified in order to hold the subsequent layers (Ngo et al., 2018). The remaining powders can be reutilized for other occasions. In order to obtain desirable mechanical properties, it is necessary a post treatment such as heating or photo-curing. Most disadvantages rely on the complexity of the reactions and process and the amount of materials available, that are low and expensive (Ngo et al., 2018).

2.2.3.2. Fused Deposition Modeling

A process where the raw material is a thin filament of thermoplastic which is heated at the nozzle, reaching a semi-liquid state, and then extruded in a typical thickness of 0.25 mm. It brings advantages such as the unnecessary need for post-processing chemical treatment or resins to cure, it involves a less expensive machinery and the materials used are greatly cost effective. Its main disadvantage relies on the inability to obtain a thickness lower than 0.25 mm and the limited number of thermoplastics available for this process. The mechanical properties of the final printed parts are influenced by the layer thickness, width or orientation of the filaments and air gap. However the inter-layer distortion was found to be the main cause for mechanical weakness (Ngo et al., 2018).

2.2.3.3. Selective Laser Sintering or Powder Bed Fusion

A powder is sintered or fused by the application of a carbon dioxide laser beam (Wong & Hernandez, 2012). It consists on the heating of the chamber until the almost melting point of the material and the fusing of the powder at the locations programmed by the designer. The list of materials that can be used with this process is quite vast and varied in terms of particle size: plastics, metals (requires a binder), a combination of metals, a combination of metals and polymers, a combination of metals and ceramics, composites or reinforced polymers (Wong & Hernandez, 2012). If we work with metals there's the need to prevent oxidation, performing the process in an inert gas atmosphere (Wong & Hernandez, 2012).

2.2.3.4. Laminated Object Manufacturing

It combines additive and subtractive techniques (Wong & Hernandez, 2012). The materials are provided in a sheet form that are bounded together through pressure, heat and with the support of a thermal adhesive coating. It uses a carbon dioxide laser to outline the selected design and it has advantages such as the low cost of production, the unnecessary refinement after manufacture and the need for supporting structures. Unfortunately, it creates inevitable waste and therefore low resolution in complex internal cavities (Wong & Hernandez, 2012).

2.2.3.5. Polyjet

Used to quickly develop highly detailed and accurate physical prototypes through a gel-type polymer with UV curable properties. It is used to develop high-precision physical parts, and is ideal for smaller parts, appearance models and master patterns. Identical to an ink-jet printer, the polyjet print head deposits small amounts of ultraviolet curable material on the building platform, eventually forming a single cross section of the part. An ultraviolet light attached to the print head simultaneously curing the material as it is printed (Wong & Hernandez, 2012).

2.3 Printed Patterns for Conductive Applications

In this subchapter different articles were analyzed in order to define the key concepts of the project, propose relations between them and debate the most relevant theories. This analysis grants an oriented structuring of the laboratory work, allowing a reasoned interpretation of the results.

2.3.1 Reliability of Roll-to-roll-printed, flexible electrodes for e-clothing applications

The first article analyzed was written by R. Sliz et. al. and its purpose was to collect and summarize information on the behaviour of printed flexible electrodes exposed to stress during elongation and washing. To do so, the investigating team used the roll-to-roll printing method and four commercially available paste containing silver particles. Apart

from the material, the samples were differentiated by pattern, eight different ones, as shown in Figure 4. In terms of testing, the analysis was based on the sample's behavior during 1000 cycles of 10% elongation and after a washing cycle with temperature of 40°C and speed of 1000 rpm.

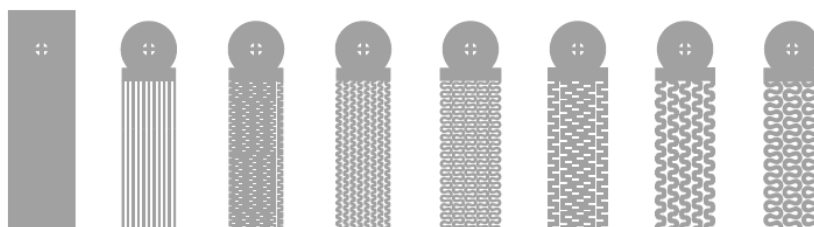


Figure 4 - 8 different patterns used by R. Silz et. al.

Before analyzing the results, the authors defined success as if 50% of the samples did not obtain values greater than 10 K Ω during elongation, and, for this reason, they eliminated 2 pastes, using only the remain 2 viable ones in the presentation and discussion of results.

In regard of the results, they noticed that, as anticipated, the resistance increased under stress, during elongation, but it also increased significantly with each cycle measured. In terms of structures, the difference between them is not noticeable, however, larger widths exhibit better endurance and the difference between the resistance during elongation and relaxation was the lowest (Sliz et al., 2020).

The samples that had better mechanical results, at cost of lower conductivity, were the samples with smaller silver flakes ($\sim 4\mu\text{m}$ and $7\mu\text{m}$) because, even though, the larger particles keep the distance of the electrodes lower, they are more prone to flake off and/or create larger voids due to elongation cycling and washing (Sliz et al., 2020).

To assess their washing behavior, the samples were submitted to a washing cycle, and their performance decreased substantially. A possible explanation for the decrement of resistance might be hidden in the washing cycle itself. The cycle introduces substantial mechanical stresses to the electrodes, and the water and detergents wash away any

particles that are not fully immobilized, leading to rough surfaces and cracks that increase resistance.

2.3.2 Printable stretchable silver ink and application to printed RFID tags for wearable electronics

Another relatable research on printable stretchable silver ink and application to printed RFID tags for wearable electronics was written by T. Zhong, et al. In this article, a comparison of electrical properties was made between an ink produced by the authors and two other commercial inks. The printing method used was screen printing and the printed design was a set of 3 straight lines 100mm long (Figure 5). The three inks were subjected to cyclical bending and stretching conditions and an analysis of the resistance variation in relation to the sintering temperature was made.



Figure 5 - Screen printing pattern used by Zhong et. al.

With reference to the sintering analyses, the samples were cured in 8 different temperatures, from 80 to 150°C with 10°C intervals at a fixed sintering time of 20 minutes. This assay made it possible to conclude that as the temperature rose, the resistivity of the material decreased.

During the bending analysis, the relative resistance of the elastic silver ink increased slowly and only about 50% after 2000 bending tests. Additionally, in the stretching test, the samples resistance was measured at rest and with +5, +10, +15 and +20% of its original size. The commercial inks used did not have a satisfactory behavior, showing no

resistance after +5 and +10% of stretching. Contrarily, the stretchable ink shown resistance through all the test and the results obtained are shown in Table 1.

Table 1 - The resistance of the produced screen-printed stretchable ink of article 2 (Zhong et al., 2019)

0%	5%	10%	15%	20%
7,1 Ω	18,4 Ω	30,9 Ω	56,9 Ω	139,0 Ω

By analysing the table above, it is possible to observe that, at maximum strain the samples shown a resistance of 139,0 Ω . It was also noticed that after removing the strain, the relative resistance recovered to a stable state in a few minutes, proving that the recovery process is time dependent.

Some hypothesized arguments for the better results obtained with the manufactured ink were the larger size of the flakes, which increased the contact area between them and therefore, formed an electrically conductive path by direct contact of adjacent silver flakes and the dispersant used, this helped to disperse silver flakes thoroughly and ensure uniformly stacked structures in the printed layer.

2.3.3 Bending reliability of printed conductors deposited on plastic foil with various silver patterns

In the research developed by T. Happonen, T. Ritvonen, P. Korhonen et al., the goal is to analyze the bending reliability of printed conductors deposited on plastic foil with three commercial silver inks and, to do so, the results were divided into three distinct parts: resistance at rest, resistance when bending and surface characterization. Two printing methods were used, roll-to-roll with a curing temperature of 140°C for 2 minutes and screen printing, cured at 250°C for 20 minutes.

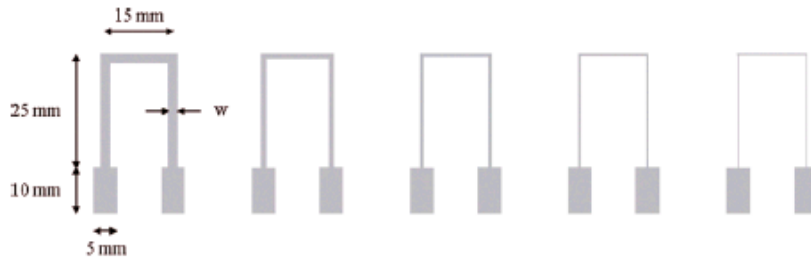


Figure 6 - Set of 5 patterns printed by T. Happonen, T. Ritvonen, P. Korhonen et al.

Apart from the differences in sample production, it is important to note that an extra set of samples was produced through roll-to-roll and subjected to annealing. Thus, three set of samples were subjected to analyses.

By interpreting the outcome of the resistance at rest, it was recognized that the samples printed with the roll-to-roll technique showed resistance values slightly higher than the screen printing samples. However, the post-annealing treatment had a remarkable effect on the nominal resistances of roll-to-roll printed specimens (Happonen et al., 2016), noting a decrease of about 30% comparatively with the non-treated ones, a lower value than those obtained through screen printing. Additionally, through analysis of the standard deviation, it was observed that the three samples obtained high similarity in terms of uniformity.

At last, three conclusions about the general reasons for the behavior of the samples at rest were made. Since the paste that had smaller silver particles was the one that obtained higher resistance values, it is possible that the smaller contact area between them influence the resistance, resulting in lower conductivity of the printed trace. However, another set of samples also had poor results and the probable cause was related to the cross-section area. The samples had a deformed geometry, they were highly widened and flattened. Lastly, the heat-treatment proved to be important for electrical characteristics and the method that obtained the highest resistance values was roll-to-roll with post-annealing.

2.3.4 General Conclusions

The three articles presented on this sub-chapter had relevant data on flexible conductive traces that can be used in textiles or similar surfaces. The methodology and results collected from the different teams provided support on the expectations and predictions of the practical work made on this dissertation. Briefly, the compiled conclusions are that, even though there are no significant differences between patterns, the structures with larger shapes (bigger width) have better endurance. As expected, resistance increases with washing due to mechanical and forces. And traces with smaller cross-sectional area have higher values of resistance. In terms of silver flakes particle size, the pasts with smaller flakes presented better values of resistance at rest but, because off their size, were prone to crack and had worse mechanical behavior.

2.4 Electrical Properties

This subchapter was incorporated in this dissertation project to illustrate the expectations though the experimental research. To do so, a basic review of Ohm's law and Gauge factor is presented.

2.4.1 Ohm's Law

Ohm's law represents a relation between current, voltage and resistance. An electric circuit is formed when a conductive path is created to allow electric charge to continuously move. This continuous movement of electric charge through the conductors of a circuit is called a current, and it is often referred to in terms of "flow".

A simplified equation to describe Ohm's law is presented in Equation 1, where I refers to current through the conductor (A), U to the voltage measured across the conductor (V) and R to the resistance of the conductor (Ω).

Equation 1 – Ohm's Law

$$I = \frac{U}{R}$$

In terms of conductive traces, another equation is used to measure the linear resistance, since there are some variables that need to be attended. This is described in Equation 2, where ρ refers to the electrical resistivity of the material (Ω/m), l to the length of the trace (m) and A to the cross-sectional area (m^2).

Equation 2 – Resistance of a conductor

$$R = \rho \frac{l}{A}$$

By analyzing this equation, some results of the experimental analysis can be predicted. Since the resistivity is a fundamental property of a material, only the cross-sectional area and the length of the trace can influence the resistance of the same. Thus, if the cross-sectional area is constant, the resistance increases if there is a length increment. On the other hand, if the area is increased and the length of the trace is maintained, the resistance decreases. This observation predicts that, for the same length, the larger the nozzle used, the lower the resistance of the conductor.

3 METHODOLOGY

Before the start of the practical component of this study, the methodology and the specific conditions of analysis were established in order to systematize the resistance values of conductive structures produced with a 3D printer.

The collected data is primary and was obtained through the control and manipulation of variables. Although there are other variables to consider, only the cross-sectional area and the printing patterns were altered, both the conductive paste and the curing temperature remained unchanged.

Some studies have already been carried out addressing similar topics and, therefore, the methodology used was based primarily on the study carried out by R. Sliz *et al.* (Sliz *et al.*, 2020)

Since this study is not a real simulation of the conditions and materials, we cannot conclude with certainty whether at the end of this project the samples are ideal or not to produce e-textiles. However, this methodology allows the evaluation of the interactions between certain controllable variables and serves as a guide for future work.

3.1 Preparation of Samples

After a scrutinized selection process, the Procusini machine was selected for the samples production. Procusini is a 3D food printer that automatically shapes a selected paste into the chosen design layer by layer, similarly to the FDM process. Since its software is capable of printing more materials other than food, it was used to print the prepared conductive paste. The operating principle of this machine is quite simple. The selected paste is inserted into a tube of fixed dimensions which is then placed into the machine. When printing, there is a mechanism that presses the paste and pushes it through the nozzle at a constant speed.

As for the support structure, a polyurethane based film, *Platilon® U 9122*, was selected (data sheet available in attachments). This substrate was selected to portray the elastic properties of a textile, offering a smooth and uninterrupted surface. In an early stage of

development, this material is ideal as it offers the elasticity of a fabric without the disadvantage of roughness and space between threads.



Figure 7 – Procusini machine

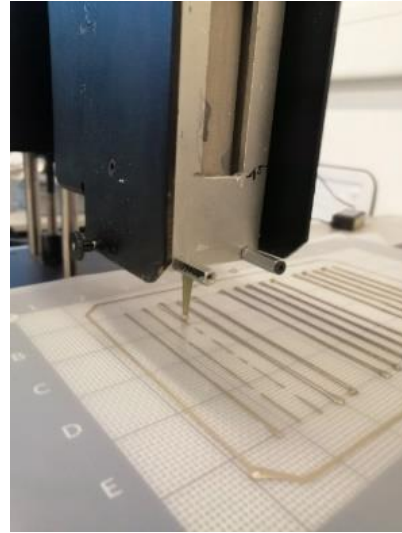


Figure 8 - Procusini producing samples

For the production of the first samples, a silicone paste with a proportion of 1:1, of *Elastosil® 6200 A* and *Elastosil® 6200 B* was used. Since the paste easily created air bubbles, and this would make it difficult to produce uniform samples, their removal was carried out in a vacuum to allow a bubble-free printing. At first, several attempts were made in order to achieve the ideal printing settings, however, due to the viscosity of the paste it became quite difficult to find the configurations that would prevent the accumulation of silicone at the ends of each pattern (Figure 9).



Figure 9 - Accumulation of silicon at the end of the printed lines

Another problem associated with air bubbles arose during the prototyping. In the printing process, air bubbles were being created and therefore causing interruptions in the printing process. To solve this problem, an alternative screw was used, this was printed at the laboratory by another 3D printer and its design included a hole like shown in Figure 10 and 11. Unsuccessfully, this approach did not exhibit positive results since the paste also passed through the hole intended only for air bubbles.



Figure 10 - Alternative screw top view

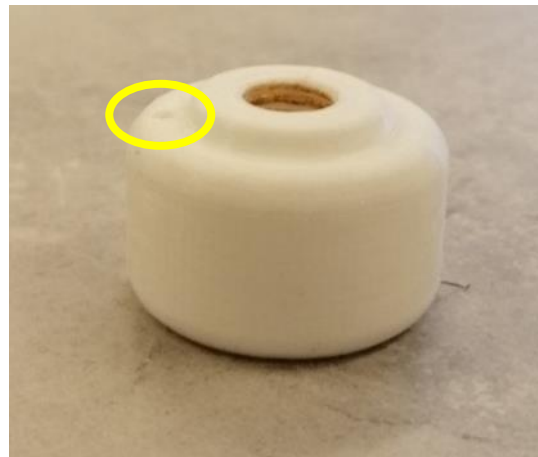


Figure 11 - Alternative screw front view

In order to overcome the situation, a new paste was prepared containing glass flakes coated with silver flakes. The recipe for this paste, which is shown in Table 2, was based on the study made by E. Lempa *et al.* (Lempa et al., 2019)

Table 2 - Recipe for the conductive paste

<i>Tubicoat PU</i>	<i>eConduct glass 352000</i>	<i>H₂O</i>	<i>Verdicker Tubicoat LP</i>
30g	27g	60g	2g

This recipe consists of a binder, which allows a cohesive connection between the other components (*Tubicoat PU*), a thickener, which increases the viscosity of the solution without significantly changing its properties (*Verdicker Tubicoat LP*), glass particles coated with silver, to provide conductivity to the paste (*eConduct glass 352000*) and water.

The simple specifications for each of the components were also acquired in the paper written by E. Lempa *et al.* and are presented in Table 3.

Table 3 - Specifications of the different components of the conductive paste

<i>Tubicoat PU</i> (<i>Polyurethane aqueous dispersion</i>)	<i>60% solid content</i>
	<i>Density of 1,08 g/cm³</i>
	<i>pH of 6,0 – 7,8</i>
<i>Verdicker Tubicoat LP</i> (<i>Polyacrylate aqueous dispersion</i>)	<i>60% solid content</i>
	<i>Density of 1,10 g/cm³</i>
	<i>pH of 7,0 – 9,0</i>
<i>eConduct glass 352000</i>	<i>Ag content of 18,5 – 21,5%</i>
	<i>Particle's size of 17 μm</i>

The ideal settings were more easily achieved using the new paste, resulting in slightly different values from pattern to pattern. The samples were printed using two nozzles with distinct sizes, 0,84 and 1,19 mm. The settings for each nozzle are presented in Table 4.

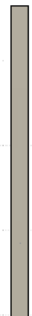
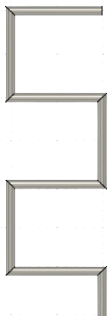
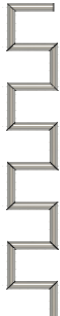


Table 4 - Settings for the printing

	Nozzle A					Nozzle B				
	1	2	3	4	5	1	2	3	4	5
Nozzle Diameter	0,84 mm					1,19mm				
Extrusion Multiplier	0,1	0,1	0,1	0,08	0,08	0,1	0,1	0,08	0,08	0,08
Retraction Distance (mm)	0,5	0,5	0,5	0,5	0,5	0,5	0,5	0,5	0,5	0,5
Retraction Vertical Lift (mm)	2,0	2,0	2,0	3,0	3,0	3,0	3,0	3,0	3,0	3,0
Retraction Speed (mm/min)	600	600	600	600	600	600	600	600	600	600
Coating Distance (mm)	3,0	3,0	3,0	3,0	3,0	3,0	3,0	3,0	3,0	3,0
Primary Layer Height (mm)	0,5	0,5	0,5	0,5	0,5	0,5	0,5	0,5	0,5	0,5
Top Solid Layers	1	1	1	2	2	3	3	2	2	2
Bottom Solid Layers	5	5	5	1	1	1	1	1	1	1

Some definitions, like extrusion multiplier, affect the final result more than others. The extrusion multiplier controls the amount of filament that comes out of the nozzle. A multiplier of 1 equal to 100 % and small adjustments in this setting can make a difference in the resolution of the final print. The retraction settings control the quantity of paste that leaves the nozzle during “non-printing” actions, like gaps or interrupted surfaces in the model, or in other words, when the nozzle is retracted. The solid layers settings influence the adhesion of the filament or paste in the substrate by applying extra pressure, heat and surface area.

The patterns were created using the software *Fusion 360* by *Adobe Autodesk*. The structure of the designs was based on three geometric models, linear, rectangular and circular. The last two patterns have a normal and smaller version, varying the width from 1 cm to 0,5 cm. A simple outline of each is shown in Table 5. 30 samples were printed for each design and nozzle.

Table 5 - Schematic of the 5 patterns

Lines (1)	Larger Rectangular (2)	Smaller Rectangular (3)	Larger Circular (4)	Smaller Circular (5)
				

The printed samples were subjected to a 70 °C curing for 10 minutes followed by the application of a protective silicone layer. The silicone paste used was the same as the one used for the first samples at the beginning of this work. This process was done manually using the *K Hand Coater* from *RK Printcoat Instruments*, obtaining, ideally, a 0,08 mm layer of silicone. Additionally, after applying the coating layer, the samples were cured again at 120 °C for 10 minutes. A simple scheme of all stages of sample production is represented in Figure 12.

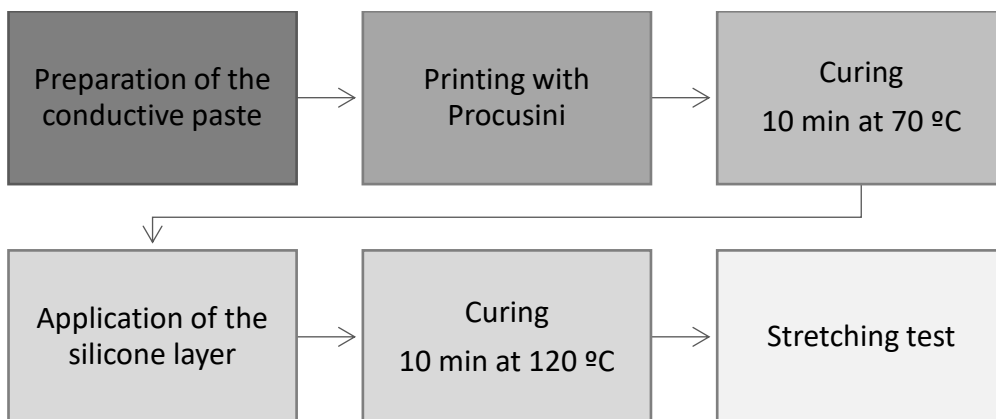


Figure 12 - Schematic of the methodology

3.2 Methods of Data Collection

As previously mentioned, the validation of the samples was done through the analysis of its electrical resistance. In order to mimic the textile purpose of the samples, they were subjected to stretching forces through the *Resistomat Burster* and to a domestic washing machine cycle.

The *Resistomat Burster 2316* is a milliohmmeter that allows fast and accurate measurements of the smallest resistances. This device is designed for both laboratory and heavy industrial use.

The maximum extension evaluated was 10 % of the sample original size and the electrical resistance was measured incrementing 1% after each reading until reaching 10%, and then decrementing 1 % back to 0 %. From each set, ten samples were selected for evaluation. As seen in Figure 13 and 14, a fragment of sanding paper was used to prevent the samples from slipping of the claw.

The elongation cycle can be divided into elongation and relaxation. In the first case, the sample was under stress and its resistance increased, and naturally, during relaxation, its length came to its initial state, the resistance decreased but not to its original value.

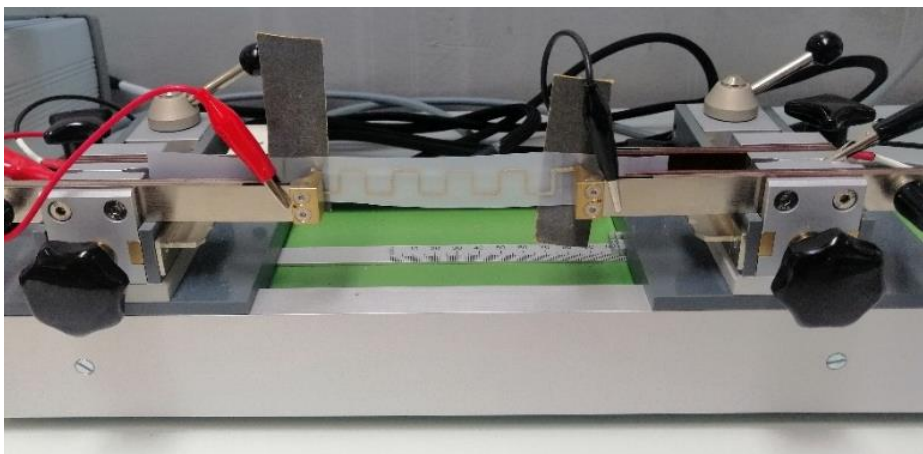


Figure 13 - Resistomat Burster 2316 while measuring a sample

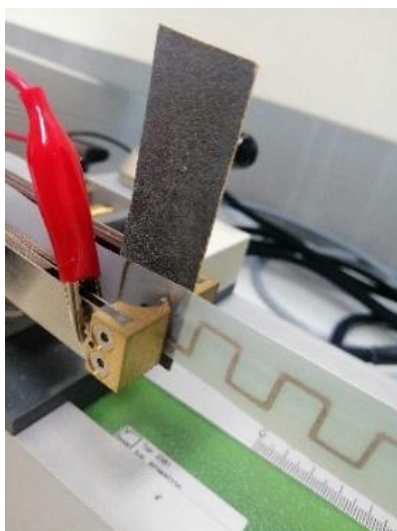


Figure 14 - Sample holding

Following, the samples were submitted to a washing cycle, using a washing machine with front loading and horizontally rotating drum, based on the standard of the DIN EN ISO 6330:2013-02 (German standard). The process was made without additional cargo during the washing cycle and without standard detergent, instead mild detergent for sensitive and fine textiles was selected. Finally, the washing program was based on the washing process “3M”, this is 15 min at 30 °C.

4 RESULTS AND DISCUSSION

In this chapter, the results collected in the project's experimental phase will be presented and discussed. However, before beginning the discussion of the results itself, a characterization of the samples was made. This characterization was supported by the images obtained by the SEM microscope and the optical microscope.

4.1 Characterization of the Samples

In the interest of complementing the information of the experimental component, the samples were analysed on a microscopic scale using a SEM microscope and an optical microscope. This analysis took place before and after having a protective silicone layer and before and after washing. With the calculation of the cross-sectional area and the actual length of the samples, it was also possible to calculate the theoretical resistance value of the samples.

4.1.1 Silver Flakes Dimensions Values

Although it is possible to distinguish several silver flakes in different collected images, the sample before applying the silicone layer was selected to calculate the flakes size. This selection was based on the clearness of the image when compared to the others. Figure 15 represents a x50 amplification in the SEM microscope and has seven flakes differentiated from the others. These seven flakes were selected to calculate the area and this calculation was made using the scale provided by the microscope, which is at the lower right end of the image.

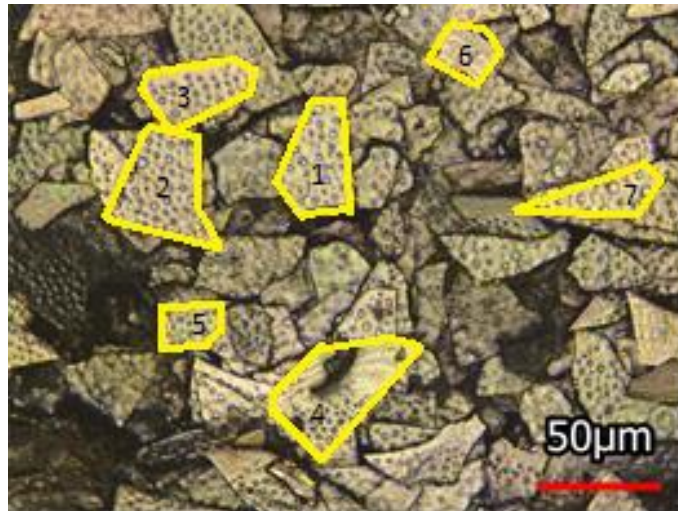


Figure 15 - x50 amplification of a linear sample with 7 flakes differentiated

The obtained areas were as follows:

- $A_1 = 977,71 \mu m^2$
- $A_2 = 1264,72 \mu m^2$
- $A_3 = 784,31 \mu m^2$
- $A_4 = 1699,63 \mu m^2$
- $A_5 = 328,13 \mu m^2$
- $A_6 = 280,0 \mu m^2$
- $A_7 = 343,75 \mu m^2$

The flakes selected have different shapes to represent the diversity of flakes present in each sample. Thus, considering the seven selected areas, it was obtained an average value of $811,18 \mu m^2$ for the flakes size.

4.1.2 Cross-sectional Area of the Printed Samples

A set of five linear samples from each nozzle was cut vertically in relation to the samples length to measure its cross-sectional area. This measurement took place directly in the optical microscope, as shown in Figure 16. It is also possible to see the applied silicone layer in the image below.

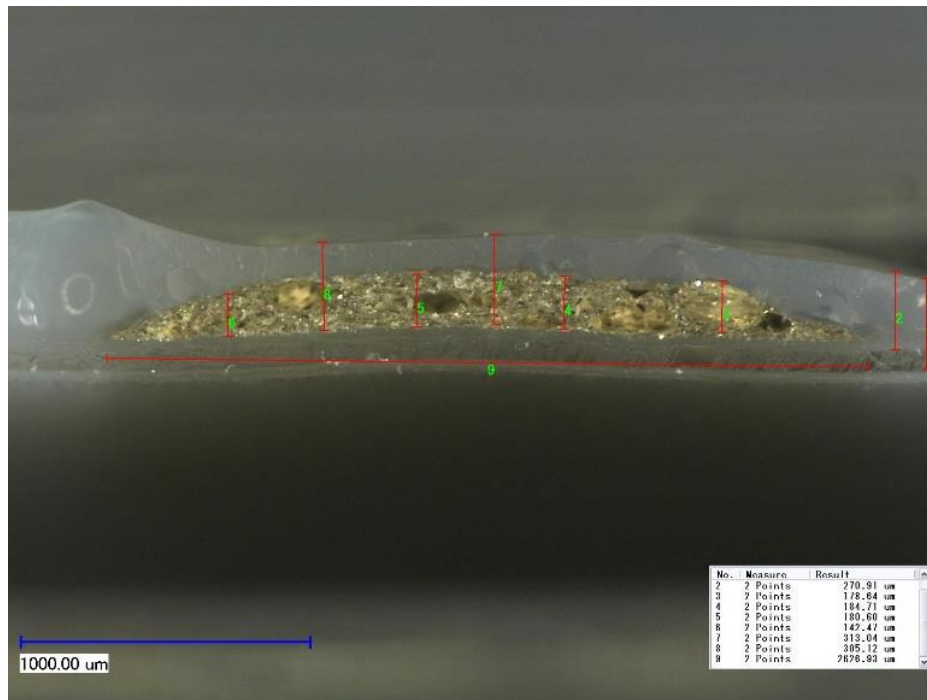


Figure 16 – Example of a x100 amplification of the cross-sectional area of a linear sample with silicone

The calculation of the area was hampered by the irregularity of the samples which, although similar in some cases, did not behave like a circular segment or any other regular shape. Thus, for each sample, an outline was created using the measurements obtained in the microscope and considering the scale defined by it. These models were created in the *Fusion 360* which automatically calculated, through the length of the different segments of the outline, their total area. Figure 17 and 18 show the models of the cross-section area of the ten analysed samples. To simplify, samples 1 to 5 refer to the 0,84 mm nozzle and samples 6 to 10 to the 1,19 mm nozzle.

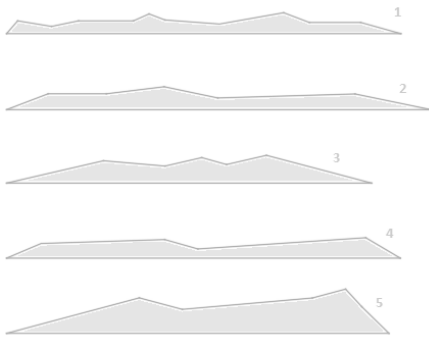


Figure 17 - Cross-sectional area of nozzle A samples

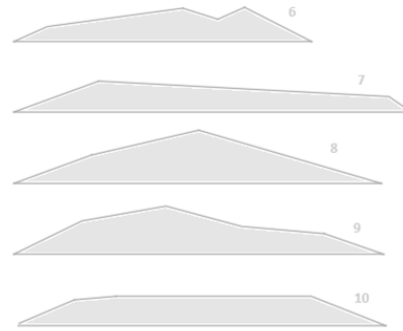


Figure 18 - Cross-sectional area of nozzle B samples

The corresponding areas are:

- $A_1 = 0,053 \text{ mm}^2$
- $A_2 = 0,065 \text{ mm}^2$
- $A_3 = 0,067 \text{ mm}^2$
- $A_4 = 0,063 \text{ mm}^2$
- $A_5 = 0,109 \text{ mm}^2$
- $A_6 = 0,319 \text{ mm}^2$
- $A_7 = 0,418 \text{ mm}^2$
- $A_8 = 0,515 \text{ mm}^2$
- $A_9 = 0,500 \text{ mm}^2$
- $A_{10} = 0,437 \text{ mm}^2$

Thus, the average area of the samples value is $0,0714 \text{ mm}^2$ for nozzle A and $0,438 \text{ mm}^2$ for nozzle B.

4.1.3 Theoretical Resistance Values for the Produced Paste

To predict the average resistance value of each set of samples, a calculation of the theoretical resistance value of the produced paste was conducted. To do so, the equation for conductive traces, Equation 2, was used.

$$R = \rho \frac{l}{A} \quad (\text{Equation 2})$$

An important aspect to consider is the percentage of silver in the paste. Analyzing the recipe, it can be noticed that the amount of eConduct glass used was 27 g and that the percentage of silver in this component varies between 18.5 and 21.5 %. Considering that the percentage of silver in the eConduct glass is 20 %, there is only 5,4 g of silver in the applied paste. Therefore, the percentage of silver is 4,54 %.

The corresponding variables are:

- $\rho = 1,6 * 10^{-8} * 0,0454 = 7,26 * 10^{-9} \Omega/m$
(bulk silver resistivity at 20°C)
- $l = 0,1 m$
- $A_1 = 7,14 * 10^{-8} m^2$ (nozzle A)
- $A_2 = 4,38 * 10^{-7} m^2$ (nozzle B)

Applying the variables in the equation, the final values of resistance for each nozzle are:

- Nozzle A:

$$R_1 = 7,26 * 10^{-9} * \frac{0,1}{7,14 * 10^{-8}} = 0,010 \Omega$$

- Nozzle B:

$$R_2 = 7,26 * 10^{-9} \frac{0,1}{4,38 * 10^{-7}} = 0,0017 \Omega$$

4.1.4 Length of the Samples

Considering that one of the goals of this study was to evaluate the influence of the pattern on the resistance of the samples, the results were recalculated for the same length, 10 cm. To do so, the actual length of the samples was calculated. In the rectangular samples, a simple addition operation allowed to reach its authentic value, however, for the circular samples, more laborious calculations were made.

Length of an Arc of a Circle

The length of an arc of a circle, L , with a radius r and subtending an angle θ is measured by:

$$\frac{L}{2\pi r} = \frac{\theta}{2\pi}$$

Since the length divided by the circumference is equal to the radian angle of the arc divided by 2π , the simplified formula is:

$$L = \theta \times r$$

So, applying the theoretical values, the size of the arc is:

- A4 and B4 Pattern $\frac{L}{2\pi \times 0.2} = \frac{90}{360} \Leftrightarrow L = 0.314 \text{ cm}$

- A5 and B5 Pattern $\frac{L}{2\pi \times 0.1} = \frac{90}{360} \Leftrightarrow L = 0,157 \text{ cm}$

Final Length of the Samples

As it would be impractical and not very realistic to measure these values directly on the samples, their theoretical values were used as their true values. The theoretical lengths of each of the samples is shown in Table 6.

Table 6 - Theoretical lengths values of the samples

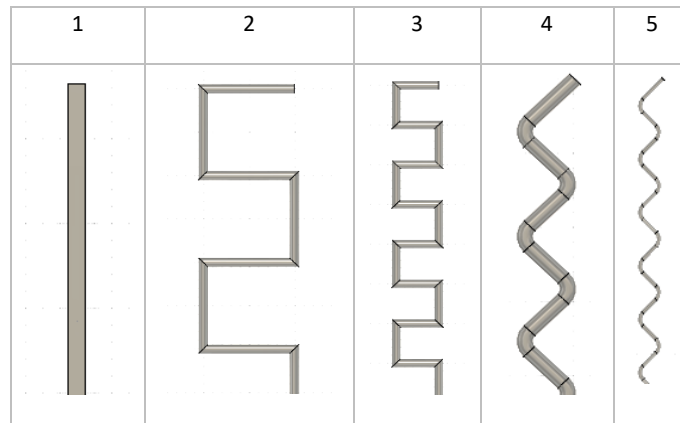
1	2	3	4	5
10 cm	21 cm	20,5 cm	12,88 cm	11,01 cm

4.2 Results from the Stretching Analysis

In this subchapter the results were organized in linear, rectangular and circular samples. However, apart from the linear, the results were also divided according to the repetition model, differentiating samples with a broader repeat cycle from those with a shorter repeat cycle. The nomenclature used to differentiate and simplify the exposure of the results was:

The samples A were produced with a 0.84 mm nozzle and B with a 1.19 mm nozzle. The samples were then divided from 1 to 5 where 1 represents the linear samples, 2 the wider rectangular samples, 3 the narrower rectangular samples, 4 the larger circular samples and 5 the smaller circular. This nomenclature is represented in Table 7.

Table 7 - Simplified nomenclature for the different patterns



In all cases, the results are presented before and after washing and all are expressed in ohms (Ω). Since the five set of samples all have different lengths, a recalculation of the results was done so that all the values corresponded to the length of 10 cm.

The definition of success established for this study was that 50 % of the samples should withstood the stretch until and at 10 %. Table 8 shows the percentage of each set of samples that enabled a reading of the resistance value throughout the entirety of the tests.

Table 8 - Reliability analysis of all samples before and after washing

	Reliability analysis	
	Before Washing	After Washing
A1	40%	40%
B1	60%	50%
A2	90%	70%
B2	70%	70%
A3	80%	70%
B3	90%	80%
A4	100%	90%
B4	100%	100%
A5	90%	90%
B5	90%	90%

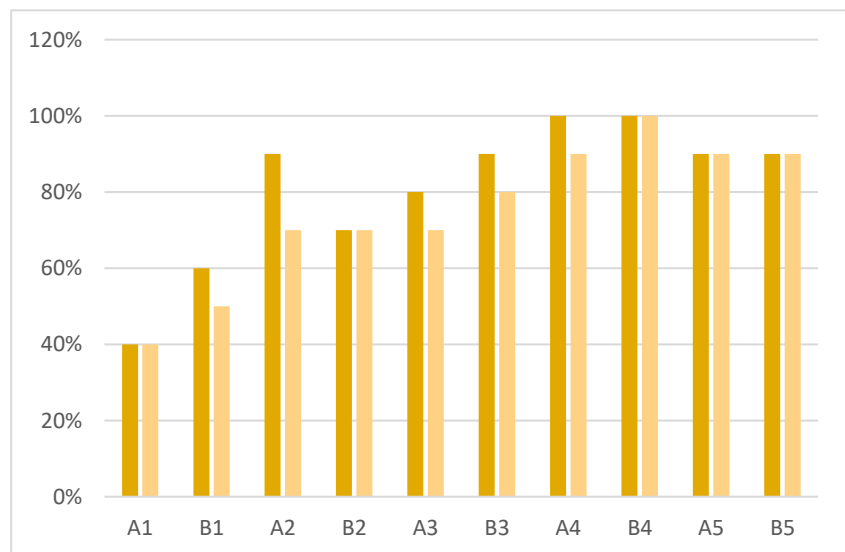


Figure 19 - Reliability analysis of all samples before and after washing

As it was expected, the samples, overall, demonstrated a lesser or equal reliability to endure the maximum stretch once exposed to the washing cycle. Looking closely, it is a straightforward conclusion that the circular design outperforms the remaining patterns and in contrast, the linear samples are the least reliable.

The A1 samples were the only batch that was deemed as unsuccessful, for the previous 50 % set value was not achieved. Oppositely, the B4 batch had a 100 % performance during the testing.

4.3 Printing Trials of the Linear Patterns

4.3.1 A1 samples

In a first analysis of Table 9, it is verified that the resistance of the samples increases significantly after being subjected to the washing operation, going from a rest value of 37,5 Ω to 3380 Ω . The maximum value obtained, before washing, is 9656 Ω at 10 %, and as anticipated, this value was reached at a lower percentage, between 4 % and 5 % in the samples after washing. In these conditions, the new maximum value is 172220 Ω , also obtained at 10 % and the percentage of resistance lost is 1683,6 %.

Table 9 - Results from stretch testing of A1 samples

A1											
	Before washing		After Washing				Before Washing		After Washing		
	\bar{x} (Ω)	σ	\bar{x} (Ω)	σ	% Loss		\bar{x} (Ω)	σ	\bar{x} (Ω)	σ	% Loss
0%	37,5	31,0	187,5	42,7	400,0	9%	3380,0	5653,8	94362,5	33746,0	2691,8
1%	45,0	23,8	320,0	89,8	611,1	8%	1037,5	1341,9	60980,0	34405,4	5777,6
2%	75,0	23,8	585,0	173,1	680,0	7%	322,5	92,2	21937,5	9632,9	6702,3
3%	112,5	17,1	837,5	187,0	644,4	6%	280,0	147,6	26457,5	19975,4	9349,1
4%	187,5	40,3	4817,5	5666,8	2469,3	5%	177,5	20,6	7047,5	5637,6	3870,4
5%	272,5	33,0	31780,0	20351,3	11562,4	4%	152,5	20,6	6900,0	5255,1	4424,6
6%	402,5	68,0	29880,0	16480,4	7323,6	3%	122,5	17,1	2292,5	2170,1	1771,4
7%	597,5	65,5	43202,5	22225,9	7130,5	2%	95,0	17,3	1300,0	739,7	1268,4
8%	2167,5	1597,1	88727,5	42554,1	3993,5	1%	80,0	14,1	577,5	236,0	621,9
9%	6275,0	4898,1	145927,5	27946,3	2225,5	0%	70,0	14,1	482,5	206,8	589,3
10%	9656,0	8185,3	172220,0	15237,6	1683,6						

This increase of resistance is expected to happen in all samples after washing like it was discussed in subchapter 2.3. It can be also noticed that the samples do not present homogeneous values between them, with cases in which the standard deviation had values of 8185,3 and 27946,3, for example.

4.3.2 B1 samples

As seen in the theoretical research, the use of a larger nozzle increases the cross-sectional area and consequently, decreases the resistance of the samples. At rest, the samples have a resistance of 16,7 Ω , a value that increases 5,5 times after being subjected to washing. The maximum value was reached, in both situations, at 10 %, being 1078,3 Ω in the first case and 66718 Ω in the second.

Table 10 - Results from stretch testing of B1 samples

B1											
Before washing		After Washing			Before Washing		After Washing				
\bar{x} (Ω)	σ	\bar{x} (Ω)	σ	% Loss		\bar{x} (Ω)	σ	\bar{x} (Ω)	σ	% Loss	
0%	16,7	5,2	92,0	35,6	81,9	9%	360,0	139,4	29074,0	19930,9	98,8
1%	26,7	5,2	110,0	40,6	75,8	8%	221,7	57,8	12466,0	12990,1	98,2
2%	38,3	7,5	156,0	61,1	75,4	7%	153,3	43,7	11326,0	13637,8	98,6
3%	55,0	8,4	260,0	144,0	78,8	6%	123,3	28,0	3710,0	5350,6	96,7
4%	83,3	16,3	350,0	189,7	76,2	5%	100,0	20,0	1232,0	1629,7	91,9
5%	116,7	35,6	632,0	372,8	81,5	4%	81,7	13,3	404,0	149,8	79,8
6%	156,7	23,4	3390,0	3080,0	95,4	3%	66,7	10,3	362,0	199,5	81,6
7%	210,0	37,9	10762,0	11606,6	98,0	2%	53,3	5,2	516,0	711,2	89,7
8%	298,3	75,5	20726,0	23995,0	98,6	1%	45,0	5,5	238,0	155,3	81,1
9%	438,3	133,5	41826,0	25287,3	99,0	0%	38,3	7,5	206,0	104,5	81,4
10%	1078,3	912,3	66718,0	30804,6	98,4						

4.3.3 Comparison of the Linear Samples Printed with the Two Nozzles

Visual analysis of the samples helps to understand the obtained values. By comparing the samples of each nozzle, it is noticeable that those printed with the 1,19 mm nozzle presented a more robust line than the samples printed with the 0.84 mm nozzle,

therefore presenting a lower resistance value, even in the after washing situation. This outcome might be explained by the higher amount of silver flakes in the B1 samples due to the greater volume of paste. Contrary to what can be seen in A1 samples, the percentage of resistance lost in samples B1 never exceeds 100, showing a more solid performance.



Figure 20 – A1 samples



Figure 21 – B1 samples

4.4 Printing Trials of Larger Rectangular Pattern

4.4.1 A2 samples

With reference to Table 11, the resting resistance value is $19,2 \Omega$ before and $141,5 \Omega$ after washing. In both cases, its maximum value occurs at a 10 % stretch, with a value of $8192,6 \Omega$ and $52909,5 \Omega$, before and after washing, respectively. The percentage loss of resistance between both situations never exceeds 100 % but is also always higher than 80 %.

Table 11 - Results from stretch testing of A2 samples

A2											
	Before washing		After Washing				Before Washing		After Washing		
	\bar{x} (Ω)	σ	\bar{x} (Ω)	σ	% Loss		\bar{x} (Ω)	σ	\bar{x} (Ω)	σ	% Loss
0%	19,2	11,9	141,5	94,0	86,4	9%	1728,6	3339,2	36467,3	26831,2	95,3
1%	18,8	11,7	183,0	93,3	89,8	8%	347,1	645,8	25685,7	22703,1	98,6
2%	18,5	10,2	245,6	136,0	92,5	7%	118,0	222,5	18915,6	19370,7	99,4
3%	20,1	9,8	443,5	278,8	95,5	6%	61,4	63,8	13700,7	15565,1	99,6
4%	28,6	18,4	1093,9	1883,2	97,4	5%	181,5	427,0	11123,8	15166,4	98,4
5%	51,9	64,0	616,3	383,9	91,6	4%	130,7	290,7	7387,1	8696,2	98,2
6%	56,6	50,6	5574,8	4606,9	99,0	3%	37,0	18,1	4576,2	7606,8	99,2
7%	693,7	1615,7	14274,8	12329,6	95,1	2%	32,8	16,2	1717,7	1850,9	98,1
8%	2009,5	3955,6	27306,8	18418,1	92,6	1%	32,8	16,1	1031,3	1352,0	96,8
9%	4467,2	7667,9	36862,6	30329,0	87,9	0%	31,7	16,1	560,5	476,0	94,3
10%	8192,6	15535,4	52909,5	36738,5	84,5						

4.4.2 B2 samples

Unexpectedly, the resting values of Table 12 are similar in the circumstances before and after being washed, increasing only 3,1 Ω and preserving uniformity between them. In this case, the maximum value corresponds to 4432 Ω before washing and 47359,9 Ω after washing.

Table 12 - Results from stretch testing of B2 samples

B2											
	Before washing		After Washing				Before Washing		After Washing		
	\bar{x} (Ω)	σ	\bar{x} (Ω)	σ	% Loss		\bar{x} (Ω)	σ	\bar{x} (Ω)	σ	% Loss
0%	7,5	2,5	10,9	3,6	31,3	9%	1391,8	1253,9	32343,5	21775,8	95,7
1%	9,5	0,3	13,6	5,8	30,0	8%	504,1	507,5	16069,4	13617,9	96,9
2%	12,9	2,3	20,4	4,5	36,7	7%	199,3	204,9	6589,8	5683,9	97,0
3%	17,7	5,3	29,9	6,6	40,9	6%	93,2	65,9	2258,5	4128,2	95,9
4%	28,6	12,6	87,8	78,3	67,4	5%	57,1	33,0	1548,3	3065,2	96,3
5%	86,4	145,1	364,6	445,7	76,3	4%	39,5	17,8	196,6	123,3	79,9
6%	155,1	294,1	1825,9	2531,7	91,5	3%	27,2	10,2	98,6	60,4	72,4
7%	272,8	526,0	3829,3	6533,6	92,9	2%	19,7	5,1	59,9	30,8	67,0
8%	638,8	807,6	15257,1	14316,2	95,8	1%	16,3	2,5	44,9	20,5	63,6
9%	1472,1	1503,4	28789,1	16905,4	94,9	0%	15,6	3,6	32,7	9,3	52,1
10%	4432,0	4701,0	47359,9	30671,1	90,6						

4.4.3 Comparison of the Larger Rectangular Samples Printed with the Two Nozzles

As seen in the linear samples, the obtained results were also of a lower resistance value in the samples produced with the 1,19 mm nozzle. By directly analyzing the samples, it is noticeable a significant increase in the thickness of the samples and consequently an increase in the volume of paste. The appearance of air bubbles along the line appears to be lower in the 1,19 mm nozzle samples, which can be an extra reason for having the best results. During testing, the samples do not show a resistance loss greater than 50 % up to 3% of stretch and never exceed 100 % during the complete the stretching series.



Figure 22 – A2 samples



Figure 23 – B2 samples

4.5 Printing Trials of Smaller Rectangular Pattern

4.5.1 A3 samples

In Table 13, the values are respectively 36 Ω and 429,9 Ω at rest and at maximum stretch and the standard deviation goes from 28,2 to only 527,4, a lower value when compared with other samples. Once washed, they develop a value of 42,5 Ω and 7921,3 Ω at 0 % and 10 %, respectively.

Table 13 - Results from stretch testing of A3 samples

A3											
	Before washing		After Washing				Before Washing		After Washing		
	\bar{x} (Ω)	σ	\bar{x} (Ω)	σ	% Loss		\bar{x} (Ω)	σ	\bar{x} (Ω)	σ	% Loss
0%	36,0	28,2	42,5	31,2	15,4	9%	192,7	167,7	3043,2	3608,1	93,7
1%	40,2	31,5	59,2	28,1	32,1	8%	119,5	93,6	875,3	777,7	86,3
2%	44,5	36,0	80,8	55,8	44,9	7%	102,4	74,6	962,4	1509,8	89,4
3%	50,6	44,4	91,3	51,2	44,6	6%	82,3	48,6	267,6	139,5	69,2
4%	56,1	46,6	128,2	76,5	56,3	5%	67,7	47,4	239,0	110,1	71,7
5%	66,5	62,0	154,0	81,2	56,8	4%	59,8	35,7	166,6	76,3	64,1
6%	80,5	71,6	198,6	94,5	59,5	3%	55,5	33,3	126,1	64,6	56,0
7%	93,9	88,9	459,2	368,5	79,6	2%	51,2	32,4	99,0	61,6	48,2
8%	113,4	110,6	579,8	520,2	80,4	1%	48,8	30,4	87,8	58,3	44,4
9%	151,2	154,9	1547,0	900,4	90,2	0%	48,2	29,2	82,2	56,4	41,4
10%	429,9	527,4	7921,3	8777,3	94,6						

4.5.2 B3 samples

In Table 14, the after-washing results are not much higher than the before. The most likely explanation for the similarity between the results might be due to the fact that the samples got stuck together with other samples while being subjected to the washing operation, not experiencing the same damage caused by the detergents and the mechanical forces as other samples did.

Table 14 - Results from stretch testing of B3 samples

B3											
	Before washing		After Washing				Before Washing		After Washing		
	\bar{x} (Ω)	σ	\bar{x} (Ω)	σ	% Loss		\bar{x} (Ω)	σ	\bar{x} (Ω)	σ	% Loss
0%	13,0	3,4	14,0	5,2	7,1	9%	117,1	24,3	145,7	51,4	19,7
1%	19,5	4,2	25,6	10,3	23,8	8%	91,1	25,1	92,7	26,1	1,8
2%	22,2	4,3	37,8	12,2	41,2	7%	64,5	17,2	70,7	17,1	8,8
3%	28,2	4,1	44,5	14,1	36,7	6%	47,2	8,1	57,9	16,2	18,6
4%	34,1	6,0	79,3	35,6	56,9	5%	37,9	7,6	45,7	11,6	17,0
5%	48,8	7,3	84,1	25,2	42,0	4%	32,5	4,9	40,2	8,1	19,2
6%	64,5	10,8	95,7	23,7	32,6	3%	29,8	4,5	32,9	5,7	9,5
7%	81,8	14,0	112,8	25,1	27,4	2%	26,6	2,6	31,1	7,8	14,6
8%	94,9	15,8	133,5	15,4	29,0	1%	23,3	5,3	27,4	6,9	15,1
9%	116,5	13,9	167,1	19,6	30,3	0%	19,0	4,5	26,2	6,9	27,6
10%	176,7	41,6	204,3	20,1	13,5						

4.5.3 Comparison of the Smaller Rectangular Samples Printed with the Two Nozzles

The samples of Figure 24 and 32 exhibit significant visual differences. Analysing them, it is seen that the B3 are more flattened than A3, which might be the responsible factor for the small difference in the before and after-washing situation. Also, B3 samples have a relatively low standard deviation and a percentage of loss that only exceeds 50 % in the 4 % stretch, being on average 23,5 %.



Figure 24 – A3 samples



Figure 25 – B3 samples

4.6 Printing Trials of Larger Circular Pattern

4.6.1 A4 samples

In the samples presented in Table 15, the average resting value of the samples is 21 Ω and 559,2 Ω at maximum stretch. After washing, the average resting value is 29,5 Ω and at maximum stretch is 744,6 Ω . Compared to the linear and rectangular samples, B4 samples are the ones that have lower values of percentage loss between before and after washing, which could mean that they are better suited to withstand stretching forces.

Table 15 - Results from stretch testing of A4 samples

A4											
	Before washing		After Washing		% Loss		Before Washing		After Washing		% Loss
	\bar{x} (Ω)	σ	\bar{x} (Ω)	σ			\bar{x} (Ω)	σ	\bar{x} (Ω)	σ	
0%	21,0	7,4	29,5	16,7	28,9	9%	405,3	621,0	436,8	238,9	7,2
1%	24,8	8,0	41,1	20,1	39,6	8%	192,5	166,3	229,8	165,7	16,2
2%	33,4	9,0	57,5	27,9	41,9	7%	136,6	115,3	171,6	114,1	20,4
3%	47,4	26,3	73,0	31,1	35,1	6%	117,9	217,3	126,6	68,9	6,8
4%	63,7	42,2	97,8	55,5	34,9	5%	110,2	114,5	118,3	49,6	6,8
5%	93,9	88,8	135,1	83,2	30,5	4%	90,6	135,6	99,4	33,8	8,9
6%	107,9	72,0	182,5	126,1	40,9	3%	62,9	42,3	83,1	43,2	24,3
7%	155,3	153,3	201,1	92,2	22,8	2%	53,6	35,8	83,1	43,3	35,5
8%	218,2	270,7	343,2	407,5	36,4	1%	45,8	28,5	78,4	44,3	41,6
9%	339,3	400,3	576,9	774,5	41,2	0%	39,6	25,7	69,9	33,5	43,3
10%	559,2	10547,0	744,6	555,6	24,9						

4.6.2 B4 samples

When at rest, the samples have a value of 17,1 Ω which increases to 2050 Ω when stretched to the maximum, corresponding to 10 %. These values are increased after undergoing the washing operation, being 33,6 Ω at 0 % stretch and 900,6 Ω at 10 %.

Table 16 - Results from stretch testing of B4 samples

B4											
	Before washing		After Washing		% Loss		Before Washing		After Washing		% Loss
	\bar{x} (Ω)	σ	\bar{x} (Ω)	σ			\bar{x} (Ω)	σ	\bar{x} (Ω)	σ	
0%	17,1	10,2	33,6	12,9	49,2	9%	155,3	102,0	515,9	357,4	69,9
1%	24,1	13,9	46,6	19,4	48,3	8%	127,3	66,0	329,5	237,0	61,4
2%	33,4	16,4	67,3	29,3	50,4	7%	109,5	52,8	214,8	117,5	49,0
3%	48,1	28,8	96,6	43,1	50,2	6%	100,2	49,7	150,1	79,8	33,3
4%	63,7	37,3	126,8	54,6	49,8	5%	91,6	46,3	115,6	55,1	20,7
5%	80,0	51,6	153,6	70,3	47,9	4%	78,4	36,5	103,5	54,3	24,3
6%	100,9	62,5	192,4	97,1	47,5	3%	73,0	40,8	97,5	42,4	25,1
7%	139,8	109,3	243,3	106,5	42,6	2%	68,3	35,8	85,4	40,7	20,0
8%	193,3	169,3	333,0	182,8	41,9	1%	62,1	40,4	76,8	36,9	19,1
9%	201,9	128,5	458,9	273,3	56,0	0%	56,7	42,4	63,0	31,2	10,0
10%	250,0	162,7	900,6	637,8	72,2						

4.6.3 Comparison of the Larger Circular Samples Printed with the Two Nozzles

By examining the A4 and B4 samples, there seems to be only a slight increase in volume in the nozzle B samples, and for that reason the resistance values between the two nozzles are not so different. These similarities might be the result of minor production errors.



Figure 26 – A4 samples



Figure 27 – B4 samples

4.7 Printing Trials of Smaller Circular Pattern

4.7.1 A5 samples

In the A5 samples presented in Table 17 have an average resistance loss of 42 % and a maximum of 85.6 %. In this case, the maximum resistance value occurs, once again, at 10 % and corresponds to 2203.4 Ω before washing and 15324,5 Ω after washing. When compared with the A4 samples, the A5 samples show higher resistance values.

Table 17 - Results from stretch testing of A5 samples

A5											
	Before washing		After Washing				Before Washing		After Washing		
	\bar{x} (Ω)	σ	\bar{x} (Ω)	σ	% Loss		\bar{x} (Ω)	σ	\bar{x} (Ω)	σ	% Loss
0%	33,3	10,2	35,2	14,4	5,4	9%	1957,8	4498,5	7933,2	10454,3	75,3
1%	46,4	11,5	61,6	26,4	24,6	8%	475,3	366,4	3702,7	5356,7	87,2
2%	63,6	12,0	103,9	42,4	38,8	7%	317,9	176,5	1693,4	3019,2	81,2
3%	79,7	18,0	135,2	43,2	41,0	6%	222,0	48,7	521,7	372,5	57,4
4%	119,1	37,3	226,1	97,7	47,3	5%	189,7	60,2	257,3	79,7	26,3
5%	163,5	46,3	289,6	86,0	43,6	4%	159,5	42,4	207,9	59,3	23,3
6%	233,1	75,2	372,4	114,0	37,4	3%	138,3	39,3	162,5	28,2	14,9
7%	300,7	93,8	455,1	131,7	33,9	2%	118,1	34,9	159,5	44,3	25,9
8%	878,0	1496,5	900,5	270,8	2,5	1%	100,9	27,4	136,2	44,7	25,9
9%	1780,6	4921,1	4516,1	6396,3	60,6	0%	88,8	24,4	118,1	33,4	24,8
10%	2203,4	470,3	15324,5	14746,3	85,6						

4.7.2 B5 samples

The resting resistance value was respectively 18,2 Ω and 22,2 Ω , before and after washing. At their maximum elongation, the samples have a resistance of 191,7 Ω , a value that increases 167 times after undergoing the washing operation.

Table 18 - Results from stretch testing of B5 samples

B5											
	Before washing		After Washing				Before Washing		After Washing		
	\bar{x} (Ω)	σ	\bar{x} (Ω)	σ	% Loss		\bar{x} (Ω)	σ	\bar{x} (Ω)	σ	% Loss
0%	18,2	15,1	22,2	12,1	18,2	9%	178,6	106,7	15679,7	23548,5	98,9
1%	21,2	14,4	39,4	9,1	46,2	8%	136,2	65,8	8159,2	12345,8	98,3
2%	27,2	15,1	59,5	13,7	54,2	7%	110,0	42,2	1269,6	1337,3	91,3
3%	32,3	13,7	86,8	15,8	62,8	6%	88,8	28,6	662,0	625,2	86,6
4%	41,4	13,7	140,3	35,5	70,5	5%	72,7	20,8	369,4	219,5	80,3
5%	49,4	15,8	194,8	48,3	74,6	4%	60,6	14,4	247,2	121,3	75,5
6%	62,6	15,4	346,1	145,5	81,9	3%	52,5	13,5	195,8	75,3	73,2
7%	74,7	14,2	1257,4	1307,3	94,1	2%	42,4	10,2	132,2	28,8	67,9
8%	95,9	23,2	5281,1	5912,5	98,2	1%	39,4	13,6	101,9	29,4	61,4
9%	131,2	44,8	10194,8	9109,9	98,7	0%	34,3	14,9	81,7	20,3	58,0
10%	191,7	101,1	32005,2	20849,2	99,4						

4.7.3 Comparison of the Smaller Circular Samples Printed with the Two Nozzles

The samples printed with nozzle B have a higher volume of used paste when compared to nozzle A samples. As the samples do not have much difference at rest, it is likely that the loss of flakes is not noticeable when stretching does not occur.



Figure 28 - A5 samples



Figure 29 - B5 samples

4.8 General Conclusions

The following table, Table 19, shows the average resting values and at the maximum stretch values for the full set of samples.

Table 19 - Summary of resistance results

			1	2	3	4	5
			RESISTANCE (Ω)				
A	B W	R	37,5	19,2	36	21	33,3
		MS	9656	8192,6	429,9	559,2	2203,4
	A W	R	187,5	141,5	42,5	29,5	35,2
		MS	172220	52909,5	7921,3	744,6	15324,5
B	B W	R	16,7	7,5	13	17,1	18,2
		MS	1078,3	4432	176,7	250	191,7
	A W	R	92	10,9	14	33,6	22,2
		MS	66718	47359,9	204,3	900,6	32005,2

Through the analysis of Table 19, there are two direct conclusions that can be drawn. Firstly, a notorious increment of the resistance occurs on every elongation, from 0 to 10 %. Secondly, there is a substantial increase of resistance in the samples after being subjected to a domestic washing, like seen in Figure 30.

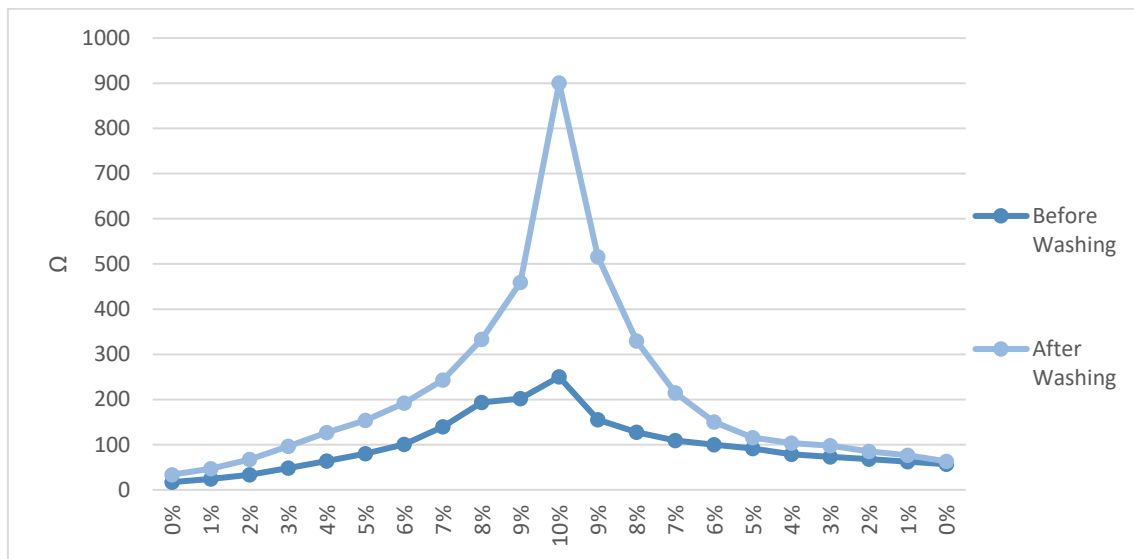


Figure 30 - Comparison of B4 samples over stretching before and after washing

B4 samples were selected as an example of a visual assessment of the increase and decrease of the resistance during testing, before and after washing.

In Figure 31 and 32, there is a comparison of the patterns for the nozzle A and B. In the first case, samples A1 and A2 show similar behaviour and resistance value. In nozzle B samples, the linear samples, B1, have a meaningful difference of resistance at maximum stretch.

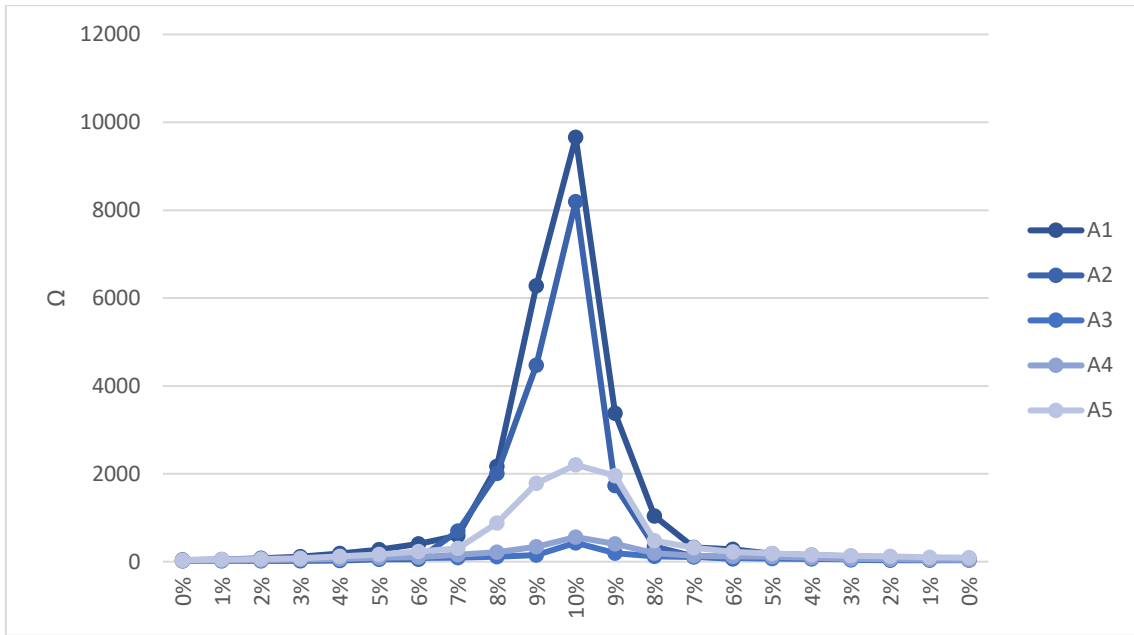


Figure 31 - Comparison between five patterns printed with nozzle A before washing

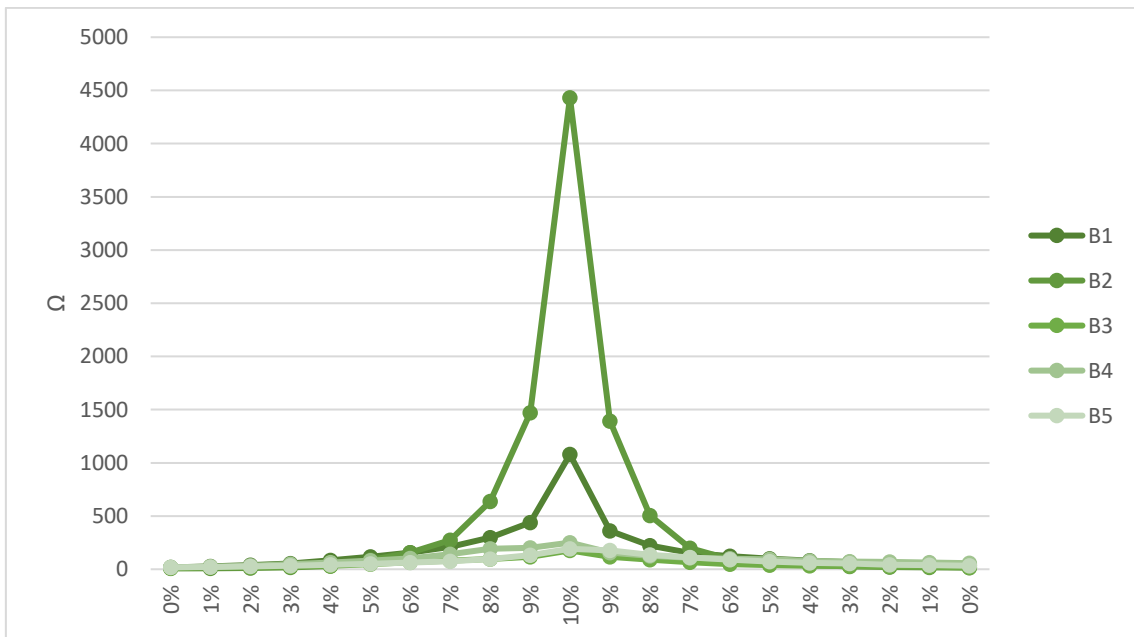


Figure 32 - Comparison between five patterns printed with nozzle B before washing

Regarding the pattern and width of the samples, it is not possible to draw a strong conclusion because two different situations happened in the rectangular and in the circular samples printed with a 1.19 mm nozzle. In the first case, the samples with greater width have greater resistance values at maximum stretch, whereas, in circular samples this occurs in the smaller width samples. Nonetheless, there is a clear improvement in the circular samples when compared to rectangular and linear ones, though deeper studies would have to be carried out to be able to draw a solid conclusion.

5 CONCLUSION

This research aimed to evaluate the influence of the cross-sectional area of several patterns on the resistance value of Stretchable and Conductive 3D Printed Sensor Structures samples when afflicted with a stretching force. The practical work consisted on the production of different sets of samples with different cross-sectional areas and five different designs, using a single conductive paste, fabricated in the chemical laboratory at the Hochschule Niederrhein.

Afore commencing the practical component of this study, it was defined as a successful sample batch if at least 50 % of the samples endured the 10 % stretch test. As it is thoroughly described in chapter 4, the samples of the same design were analysed and then compared between the two nozzles. To prevent the samples getting damaged, a silicone layer was manually applied in each set of samples. This coating was applied with the intention of protecting the samples from any external erosion, however it was necessary that the coating would not influence the sample's resistance. Hence the chosen material was silicone, for it would preserve the sample and unalter its resistance value. Once the coating was applied, the necessary measurements were conducted, by selecting a milliohmmeter, *Resistomat Burster 2316*, which directly measured the "resting" resistance and the after-stretching resistance.

As previously discussed, the set of samples would only be defined as a successful batch, if at least 50 % of the batch's samples endured the 10 % stretch test. Regarding Table 8, only one set was designated as unsuccessful (A1), as it did not meet the previously mentioned criteria. Opposingly, the B4 set was able to withstand the 10 % stretch test with 100 % efficacy. It can be also concluded, by examining the B1 batch, with a reliability of only 60 %, that the linear samples are the most prone to crack and demonstrated the most unstable behavior. There is a clear reliability distinction between the rectangular and the circular samples, the circular samples had a success rate between 90-100% while the rectangular samples vary around 70-90 %. This occurrence might have been caused by the angle of connection created between the different segments of the pattern. The rectangular samples are connected with angles of 90° while the circular samples have a smaller and less rugged arch. This difference in the connecting angles might influence

the susceptibility of emerging cracks in the paste, making the rectangular samples more prone to fail.

This study consists of several key points. The first accountable trait of the samples is the sharp resistance increment that occurs after washing. The most probable cause for the resistance accretion to take place after the washing process, is due to a detriment of silver flakes. Mainly, there are 3 factors that could cause such detriment. The induced centrifugal forces, the detergent and the water. Those factors cause the sample to lose a significant amount of silver flakes which itself, is the main “provider” of conductivity of the sample.

Looking at the theoretical research, there are a few theoretical values validated by the practical readings. According to the theoretical research, the larger the cross-sectional area, the lower the resistance of the sample and the higher the endurance, which can be confirmed by the observed practical values of the samples. At the end of the experiment, after the samples were subjected to the stretching forces, the resistance value decreased and, theoretically, should have had returned to its original value, nonetheless, neither of the samples had a resistance value close to the theoretical value assumably due to the loss of its original integrity, a deformation, provoked by the stretch.

To better understand the results, a theoretical prediction, calculated at the beginning of chapter 4, permitted a theoretical resistance value for each of the nozzles by considering the amount of silver flakes in the produced paste, the cross-sectional area of the samples and their length (which was assumed to be 10 cm). The values were 0.010 Ω in nozzle A and 0.0017 Ω in nozzle B. In none of the cases the values obtained experimentally were of the same magnitude as the expected value. The lowest case of resistance obtained was sample B2 and even this case was 4411 times greater than the respective theoretical value. This difference between values is possibly due to the errors associated with the production process, both in the manufacture of the paste which may not have an ideal flake distribution uniformity, and in the actual printing.

Although the difference in patterns is notorious when analysing its performance, in terms of resistance, the distinction is not so considerable. Focusing on the pre-wash

situation, it is not possible to conclude with certainty which design is best suited for an application of e-textiles, future studies focusing on this distinction are still necessary.

5.1 Limitations and Future Work

During this project, there were some events that conditioned its development. The biggest obstacle was the confinement experienced at arrival in Germany on the Erasmus exchange project because of the CORONA-virus. This confinement, in addition to the personal stress caused, prevented the practical component from starting in due time and the theme of the work was constantly changed given the confinement situation. A further change in the plan was made and the remaining time in Germany allowed only one month of practical work. However, the proposed new objectives were achieved.

The future work would have been realized if the project had gone on without the limitations. As it was not possible to draw a viable conclusion about the selected standards, new sets of samples would be idealized to understand the influence of the connecting angles and the size of the segments on the electrode's resistance. A third optimization of the conductive paste would be done perhaps by adding silver flakes in greater quantity or from different suppliers.

REFERENCES

- Atallah, L., Jones, G. G., Ali, R., Leong, J. J. H., Lo, B., & Yang, G. Z. (2011). Observing recovery from knee-replacement surgery by using wearable sensors. *Proceedings - 2011 International Conference on Body Sensor Networks, BSN 2011, May*, 29–34. <https://doi.org/10.1109/BSN.2011.10>
- Avnet Abacus. (2019). *Pressure Sensors: The Design Engineer's Guide*. 97. <https://www.avnet.com/wps/portal/abacus/solutions/technologies/sensors/pressure-sensors/download-guide/>
- Brinker, C. J., Frye, G. C., Hurd, A. J., Ashley, C. S., Laboratories, S. N., & Introduction, I. (1991). *97 fundamentals of sol-gel dip coating*. 201, 97–108.
- Castano, L. M., & Flatau, A. B. (2014). Smart fabric sensors and e-textile technologies: A review. *Smart Materials and Structures*, 23(5). <https://doi.org/10.1088/0964-1726/23/5/053001>
- Dearden, A. L., Smith, P. J., Shin, D., Reis, N., Derby, B., & Brien, P. O. (2005). *A Low Curing Temperature Silver Ink for Use in Ink-Jet Printing and Subsequent Production of Conductive Tracks*. 315–318. <https://doi.org/10.1002/marc.200400445>
- European Committee for Standardization. (2011). *CEN/TR 16298:2011 Textiles and textile products – smart textiles – definitions, categorizations, applications and standardization needs*. 44.
- Gnanasekaran, K., Heijmans, T., van Bennekom, S., Woldhuis, H., Wijnia, S., de With, G., & Friedrich, H. (2017). 3D printing of CNT- and graphene-based conductive polymer nanocomposites by fused deposition modeling. *Applied Materials Today*, 9, 21–28. <https://doi.org/10.1016/j.apmt.2017.04.003>
- Happonen, T., Ritvonen, T., Korhonen, P., Häkkinen, J., & Fabritius, T. (2016). Bending reliability of printed conductors deposited on plastic foil with various silver pastes. *International Journal of Advanced Manufacturing Technology*, 82(9–12), 1663–1673. <https://doi.org/10.1007/s00170-015-7403-9>
- Jaime, L. (2010). Contact Definition in Industrial Silicon Solar Cells. *Solar Energy*, February 2010. <https://doi.org/10.5772/8075>

- Lempa, E., Rabe, M., & Van Langenhove, L. (2019). *Electrically Conductive Textiles Under Consideration of Percolation Threshold and Polymer*. June, 11–15.
- Meirowitz, R. E. (2016). Coating processes and techniques for smart textiles. In *Active Coatings for Smart Textiles*. Elsevier Ltd. <https://doi.org/10.1016/B978-0-08-100263-6.00008-3>
- Merilampi, S., Laine-Ma, T., & Ruuskanen, P. (2009). The characterization of electrically conductive silver ink patterns on flexible substrates. *Microelectronics Reliability*, 49(7), 782–790. <https://doi.org/10.1016/j.microrel.2009.04.004>
- Merilampi, Sari, Björninen, T., Haukka, V., Ruuskanen, P., Ukkonen, L., & Sydänheimo, L. (2010). Analysis of electrically conductive silver ink on stretchable substrates under tensile load. *Microelectronics Reliability*, 50(12), 2001–2011. <https://doi.org/10.1016/j.microrel.2010.06.011>
- Ngo, T. D., Kashani, A., Imbalzano, G., Nguyen, K. T. Q., & Hui, D. (2018). Additive manufacturing (3D printing): A review of materials, methods, applications and challenges. *Composites Part B: Engineering*, 143(December 2017), 172–196. <https://doi.org/10.1016/j.compositesb.2018.02.012>
- Pierson, H. O., Publishing, W. A., & York, N. (1999). *HANDBOOK OF CHEMICAL VAPOR DEPOSITION (CVD) by (Issue Cvd)*.
- Regtien, P. P. L. (2012). Resistive Sensors. In *Sensors for Mechatronics*. <https://doi.org/10.1016/b978-0-12-391497-2.00004-2>
- Shahariar, H., Kim, I., Soewardiman, H., & Jur, J. S. (2019). Inkjet Printing of Reactive Silver Ink on Textiles [Research-article]. *ACS Applied Materials and Interfaces*, 11, 6208–6216. <https://doi.org/10.1021/acsami.8b18231>
- Sliz, R., Huttunen, O. H., Jansson, E., Kemppainen, J., Schroderus, J., Kurkinen, M., & Fabritius, T. (2020). Reliability of R2R-printed, flexible electrodes for e-clothing applications. *Npj Flexible Electronics*, 4(1), 1–9. <https://doi.org/10.1038/s41528-020-0076-y>
- Tyler, D.J. (2011a). Digital printing technology for textiles and apparel. In *Computer Technology for Textiles and Apparel* (pp. 259–282). Woodhead Publishing Limited.

<https://doi.org/10.1533/9780857093608.3.259>

Tyler, D.J. (2011b). Digital printing technology for textiles and apparel. In *Computer Technology for Textiles and Apparel*. Woodhead Publishing Limited.

<https://doi.org/10.1533/9780857093608.3.259>

Tyler, David J. (2005). Textile digital printing technologies. *Textile Progress*, 37(4), 37–41. <https://doi.org/10.1533/tepr.2005.0004>

Vaezi, M., Seitz, H., & Yang, S. (2013). A review on 3D micro-additive manufacturing technologies. *International Journal of Advanced Manufacturing Technology*, 67(5–8), 1721–1754. <https://doi.org/10.1007/s00170-012-4605-2>

Wong, K. V., & Hernandez, A. (2012). A Review of Additive Manufacturing. *ISRN Mechanical Engineering*, 2012, 1–10. <https://doi.org/10.5402/2012/208760>

Zhong, T., Jin, N., Yuan, W., Zhou, C., Gu, W., & Cui, Z. (2019). Printable stretchable silver ink and application to printed RFID tags for wearable electronics. *Materials*, 12(18), 1–14. <https://doi.org/10.3390/ma12183036>

ANNEX

Polyurethane film “Platilon U 9122” Data Sheet



Product Information

Platilon® U 9122

Film based on Polyether Urethane
 Colour: natural, white, black and transparent blue
 Special characteristic: Polyether Urethane film suitable for printing and with excellent adhesion bonding properties

Typical Properties

Property	Standard / Procedure	Unit	Value
Density	calculated	g/cm ³	1,12 ¹⁾
Hardness	DIN 7619-1, DIN EN ISO 868 or ASTM D2240	Shore A	87 ²⁾
Softening Range	TMA Onset – Endset internal method	°C	160 – 190
Tensile stress at break	DIN EN ISO 527	MPa	80 ³⁾
			70 ³⁾
Tensile stress at 50% strain			6 – 10
			5 – 8
Tensile strain at break			560 ³⁾
			540 ³⁾
Tear propagation resistance	DIN ISO 34-1, B	kN/m	65 ³⁾
			65 ³⁾

These data are provided as general information only. They are approximate values and not intended for use in preparing specifications! Please contact us before writing specifications on this product.

¹⁾ Values for natural films 100 µm were calculated based on information by raw material suppliers and the film's composition.
²⁾ Based on data for the TPU resins provided by their suppliers and based on suppliers standard/procedure, not measured for film sample.
³⁾ Blown films may be orientated to a different degree depending on film thickness. The above mentioned values have been measured on natural films 100 µm and averaged over a long period. The average values from single productions can vary up to 30% subject to width and orientation.

Typical Film Dimensions

Thickness	(μm)	25 – 250
Width	(mm)	1200 – 2400 (limitations depending thickness)

Regarding thickness and width, certain interdependencies may apply. Please consult with your customer service representative. Blown film may show an orientation in either machine or cross direction. MD/CD values may vary depending on thickness and width. Our "General Conditions of Sale" also apply.

The manner in which you use and the purpose to which you put and utilize our products, technical assistance and information (whether verbal, written or by way of production evaluations), including any suggested formulations and recommendations, are beyond our control. Therefore, it is imperative that you test our products, technical assistance, information and recommendations to determine to your own satisfaction whether our products, technical assistance and information are suitable for your intended uses and applications. This application-specific analysis must at least include testing to determine suitability from a technical as well as health, safety, and environmental standpoint. Such testing has not necessarily been done by Epurex Films GmbH & Co. KG.

Unless we otherwise agree in writing, all products are sold strictly pursuant to the terms of our standard conditions of sale which are available upon request. All information and technical assistance is given without warranty or guarantee and is subject to change without notice. It is expressly understood and agreed that you assume and hereby expressly release us from all liability, in tort, contract or otherwise, incurred in connection with the use of our products, technical assistance, and information. Any statement or recommendation not contained herein is unauthorized and shall not bind us. Nothing herein shall be construed as a recommendation to use any product in conflict with any claim of any patent relative to any material or its use. No license is implied or in fact granted under the claims of any patent.



eConduct Glass 352000 Data Sheet

technical data sheet



Date of impression 18.11.2020/10:56:17
page/of 1/1

edition 15.11.2020

material denomination **eConduct Glass 352000**
material-no. 022907SG0
material description Silver coated Glass Flake

material specification

insp. characteristic	specification	unit
TI00225 Ag content	18,5 - 21,5	%
TI00288 D 10	10,0 - 20,0	µm
TI00288 D 50	25,0 - 35,0	µm
TI00288 D 90	55,0 - 65,0	µm

total shelf life in month: 24

EC-safety data sheet-no. 022907SG0

The Data on this technical information sheet correspond with the current status of our knowledge and experience.
The liability for the application and processing of our products lies with the buyer, and he is also responsible for observing any third party rights.
We reserve the right to alter any product data as a result of technical progress or further developments in the manufacturing process.

Draft	Approval	Release
Technical services	Production	Quality control
15.11.2020	15.11.2020	15.11.2020

This document has been printed automatically and will not be signed.

A member of ALTANA

Elastosil® LR 6200 A/B Data Sheet



CREATING TOMORROW'S SOLUTIONS

ELASTOSIL® LR 6200 A/B



Liquid Silicone Rubber (LSR)

Solvent-free, free-flowing, addition curing two-component silicone rubber for textile coatings

Properties

- Very low viscosity gives good penetration into the substrate
- Dry surface touch
- Well suited for flame resistant textile coatings

Technical data

Properties Uncured

Property	Condition	A	B	Method
Viscosity, dynamic ⁽¹⁾	-	20000 mPa·s	20000 mPa·s	Brookfield

¹ 2.5 rpm

These figures are only intended as a guide and should not be used in preparing specifications.

Properties Cured

Cure conditions: mixture of LR 6200 A/B in ratio 1 : 1, 5 min / 165°C

Property	Condition	Value	Method
Appearance	-	white	-
Hardness Shore A	-	40	ISO 7619-1
Density	-	1.10 g/cm ³	DIN EN ISO 1183-1 A
Tensile strength	-	2.8 N/mm ²	ISO 37 type 1
Elongation at break	-	210 %	ISO 37 type 1
Oxygen index LOI	-	31 %	ASTM D 2863
Tear strength	-	4,6 N/mm	ASTM D 624 B

These figures are only intended as a guide and should not be used in preparing specifications.

All the information provided is in accordance with the present state of our knowledge. Nonetheless, we disclaim any warranty or liability whatsoever and reserve the right, at any time, to effect technical alterations. The information provided, as well as the product's fitness for an intended application, should be checked by the buyer in preliminary trials. Contractual terms and conditions always take precedence. This disclaimer of warranty and liability also applies particularly in foreign countries with respect to third parties' rights.

Applications

- Architectural Textiles
- Flame & Heat Protection
- Textiles for Protective Clothing

Application details

ELASTOSIL® LR 6200 A/B is a liquid silicone rubber with very low viscosity to produce textile coatings with good penetration into the substrate and dry surface touch.

ELASTOSIL® LR 6200 A/B is well suited for textile coatings applications requiring enhanced flame retardancy.

Processing

ELASTOSIL® LR 6200 A/B is processed by thorough mixing of component A and B in a ratio 1 : 1.

Pot life at 23°C: 3 days

Recommended curing conditions: 3 min at 150°C or 1 min at 180°C

Adhesion of ELASTOSIL® LR 6200 A/B is generally good on nylon and polyester fabrics. It can be necessary in some cases to improve adhesion with additives (e.g. CATALYST C05 or adhesion promoters). Preliminary testing should be carried out to determine optimum formulation and cure conditions.

Packaging and storage

Packaging

This product is available in 20 kg pails and 200 kg drum kits.

Storage

Once opened, containers should always be resealed after use to prevent the platinum catalyst from being poisoned by amines, sulphur or phosphorus compounds.

The 'Best use before end' date of each batch is shown on the product label. Storage beyond the date specified on the label does not necessarily mean that the product is no longer usable. In this case however, the properties required for the intended use must be checked for quality assurance reasons.

Safety notes

Comprehensive instructions are given in the corresponding Material Safety Data Sheets. They are available on request from WACKER subsidiaries or may be printed via WACKER web site <http://www.wacker.com>.

QR Code ELASTOSIL® LR 6200 A/B



For technical, quality or product safety questions, please contact:

Wacker Chemie AG, Hanns-Seidel-Platz 4, 81737 Munich, Germany
info@wacker.com, www.wacker.com

The data presented in this medium are in accordance with the present state of our knowledge but do not absolve the user from carefully checking all supplies immediately on receipt. We reserve the right to alter product constants within the scope of technical progress or new developments. The recommendations made in this medium should be checked by preliminary trials because of conditions during processing over which we have no control, especially where other companies' raw materials are also being used. The information provided by us does not absolve the user from the obligation of investigating the possibility of infringement of third parties' rights and, if necessary, clarifying the position. Recommendations for use do not constitute a warranty, either express or implied, of the fitness or suitability of the product for a particular purpose.

TUBICOAT PU 60 Data Sheet



Preliminary Leaflet

TUBICOAT PU 60

Characterization	PU dispersion which is stable to hydrolysis
Chemical Structure	Aliphatic polyether/polycarbonate urethane
Supplied Form	White, low viscous dispersion
Ionic Character	Anionic
Active Content	Approx. 60 %
pH Value	7.0 - 9.0
Stabilities	TUBICOAT PU 60 is highly sensitive to frost; temperatures around the freezing point cause irreversible changes. TUBICOAT PU 60 is sensitive to temperatures above 40°C.
Storage	If stored in a cool place (not below 5 °C) but protected from frost, the product will hold for six months. Keep containers well closed.

The above given values are product describing data. Please consult the 'delivery specification' for binding product specifications. Further data about product properties, toxicological, ecological data as well as data relevant to safety can be found in the safety data sheet.

Properties

TUBICOAT PU 60 forms a soft, elastic, clear film which is stable to hydrolysis and adheres well on various substrates.

Application Procedure

- Since polymers always tend to drying and forming a film, the dispersion is usually filtered prior to use.
- TUBICOAT PU 60 can be used alone as synthetic dispersion. By blending it with other synthetic dispersions the film hardness, elasticity and tackiness of the film and the corresponding properties of the coating can be adjusted. Preliminary compatibility tests have to be carried out at any rate.
- TUBICOAT PU 60 is applied for textile coatings if a soft handle with a high elasticity is desired. The resulting film has a high stability to mechanical impact and a good stability to dry cleaning. With a proper crosslinking coatings produced with TUBICOAT PU 60 are excellently stable to hydrolysis. Applied as stable foam the coating has elastic recovery properties.

- TUBICOAT PU 60 can be easily thickened with disperse thickeners (e.g. TUBICOAT VERDICKER LP or TUBICOAT ASD with the addition of ammonia). If thickeners on a natural base are applied (e.g. TUBICOAT HEC), the production of a stock preparation is recommended to which the required quantity of TUBICOAT PU 60 is added.
- For achieving optimum fastnesses we recommend adding a crosslinking agent based on melamine formaldehyde (TUBICOAT FIXIERER HT) or based on isocyanate (TUBICOAT FIX H 26).
- TUBICOAT PU 60 can be applied by various coating techniques (knife, screen, spraying, foam, padding, etc.). For achieving good fastness properties the fixing temperature ought to be at least 140 °C.

Please note:

Coated textiles have to meet a defined requirement profile, which will only be possible if the basic material, the coating recipe and the processing technique are adjusted to one another.

We reserve the right to modify the product and technical leaflet.

Our department for applied technique is always at your service for further information and advice.

Our technical advice and recommendations given verbally, in writing or by trials are believed to be correct. They are neither binding with regard to possible rights of third parties nor do they exempt you from your task of examining the suitability of our products for the intended use. We cannot accept any responsibility for application and processing methods which are beyond our control.

Edition: March 2021

CHT Germany GmbH

Postfach 12 80, 72002 Tübingen, Bismarckstraße 102, 72072 Tübingen, Germany

Telephone: 07071/154-0, Fax: 07071/154-290, Email: info@cht.com, Homepage: www.cht.com

TUBICOAT Verdicker LP Data Sheet



TUBICOAT VERDICKER LP

Character	Synthetic thickener for coating pastes
Chemical Composition	Polyacrylic acid
Appearance	Slightly yellowish, slightly viscous paste
Ionic Character	Anionic
pH Value	7.5 – 8.5 (2 %)
Stabilities	TUBICOAT VERDICKER LP is highly sensitive to frost; after the impact of temperatures around the freezing point irreversible changes will occur.
Storage	If stored properly in a cool place in closed original containers, the product will hold for at least six months. The product tends to sedimenting but after thorough stirring it is ready for use again. Frost impact is to be avoided.

The above given values are product describing data. Please consult the 'delivery specification' for binding product specifications. Further data about product properties, toxicological, ecological data as well as data relevant to safety can be found in the safety data sheet.

Properties

- TUBICOAT VERDICKER LP stands out for a good thickening force
- good compatibility with anionic and non-ionic chemicals and auxiliaries which are applied within the scope of coating; preliminary trials, however, are indispensable
- good running behaviour in case of paste coatings
- requires a thorough stirring unit
- swells quickly in aqueous systems
- the coating pastes produced with TUBICOAT VERDICKER LP stand out for a rather long flowing behaviour, which only leads to a low penetration of the paste into the fabric

Application Technique

Diluting Instructions

TUBICOAT VERDICKER LP is directly stirred into the medium to be thickened. Please take care that everything is stirred thoroughly with an efficient stirring power.

Since TUBICOAT VERDICKER LP has also a retarding effect on the swelling, the desired viscosity may only be achieved after several minutes. Please ensure a sufficient stirring!

Application Fields

TUBICOAT VERDICKER LP is applied for all kinds of paste coatings within various viscosity ranges. Rheological adjustments can be realised by using TUBICOAT VERDICKER PRA, too.

Application Quantity

The application quantity depends on the paste composition and the desired viscosity and is 10 - 30 g/kg. The pH value of the paste ought to be in the neutral to slightly alkaline range and may be adjusted with ammonia if need be.

We reserve the right to modify the product and technical leaflet.

Our department for applied technique is always at your service for further information and advice.

Our technical advice and recommendations given verbally, in writing or by trials are believed to be correct. They are neither binding with regard to possible rights of third parties nor do they exempt you from your task of examining the suitability of our products for the intended use. We cannot accept any responsibility for application and processing methods which are beyond our control.

Edition: June 2012

CHT Germany GmbH

Postfach 12 80, 72002 Tübingen, Bismarckstraße 102, 72072 Tübingen, Germany

Telephone: 07071/154-0, Fax: 07071/154-290, Email: info@cht.com, Homepage: www.cht.com